

# Delineation, Specification, and Formalization of the TWZ Data Set Generation Process – Philosophical, Procedural, and Mathematical

John Sheliak

## Abstract

Elements of vector mathematics and piecewise linear analysis are used to delineate and mathematically formalize each step in the process by which the TimeWave Zero (TWZ) 384 number *data set* is generated. This development begins with the King Wen hexagram sequence and proceeds to the final 384 number data set, using standard mathematical procedures and operations. The process is clarified and streamlined by the introduction of vector notation and operations, which also preserves the notion of wave "directed" flow, described by McKenna.

This 384 number data set serves as the input data file for the TWZ software, which performs a "fractal" transform on the input data in order to produce the output *TimeWave* viewed on the computer screen as an x-y graph of *Novelty*. The basis for this data set is the first order of difference (FOD) of the King Wen sequence, defined as the number of lines that change as one moves from hexagram to hexagram, beginning at hexagram 1 and proceeding to hexagram 64. This first order of difference (FOD) number set and its derivatives are produced by a series of clearly defined mathematical operations, which are all described in detail.

Once this *revised* 384 number data set has been calculated, it is used as input to the TWZ software in order to generate *revised TimeWaves* that may be compared with the original *standard TimeWaves*. Several *random* number sets are also generated and used similarly to produce *random TimeWaves* for comparison. Fourier transform operations are performed on each of the 384 number data sets, in order to examine wave noise and information content. Correlation is used to determine the degree of interdependence between the two *data* sets, and between the data and *random* number sets.

The results of the mathematical formalization and subsequent comparison analysis show that the *revised* data set produces a *TimeWave* that appears to reflect historical process with greater accuracy than the *standard TimeWave*. This difference is likely due to the fact that the *standard* data set produces a distorted *TimeWave*, as the result of imbedded mathematical errors that increase the noise level in the wave. Comparisons of the *standard* and *revised data sets* and *TimeWaves*, show a generally high degree of correlation, inferring that the *standard wave* retains much of the information content of the revised wave, despite its distortion. This *TimeWave* information content, or the wave signal-to-noise ratio (s/n), is improved by using the revised data set, which serves to correct the noise distortion introduced by the standard wave.

## Introduction

*TimeWave Zero*<sup>1</sup> (TWZ) is a mathematical and graphical expression of the *Novelty Theory* advanced by Terence McKenna, and implemented by computer software called *Time Surfer*© for Macintosh, and *Time Explorer*© for DOS operating systems. It is based on a specific mathematical relationship exhibited by the King Wen sequence of the I-Ching – i.e. the number of lines that change as one moves from one hexagram to the next, beginning at hexagram 1 and proceeding to hexagram 64. This number set, called the First Order of Difference (FOD), was first expressed and expanded by McKenna<sup>2</sup> and others, into the TimeWave that is produced by the TWZ software. The philosophical nature and theoretical basis of the TimeWave, have been reported extensively elsewhere<sup>1</sup> and will not be discussed in detail here. However, the general thrust of *Novelty Theory*, is that information about some fundamental natural process is encoded in the I-Ching in general, and the FOD number set in particular. This process is thought to express itself in nature and the cosmos, as the ongoing creation and conservation of increasingly higher ordered states of complex form. The *TimeWave* is then viewed as expressing this process as a kind of fractal map of temporal resonance in nature, or as an expression of the ebb and flow of an organizing principle called *Novelty*.

The conversion of this FOD number set into the TimeWave (viewed on the TWZ computer screen as a graph of the *Novelty* process), involves the performance of a series of mathematical procedures and operations on this number set. The TimeWave is actually produced in two distinct and mathematically different phases. The first phase includes the creation of a simple bi-directional wave using the FOD number set. This wave is then expanded into linear, trigramatic, and hexagramatic bi-directional waves that are subsequently combined to form the *tri-level complex wave*, or 384 number data set. The second phase is performed by the TWZ software itself, which includes an expansion, or “fractal transform” of the 384 number data set (input file to TWZ) to produce the TimeWave viewed on the computer screen. Phase I uses the mathematics of piecewise linear analysis to generate the 384 number data set from the FOD number set, whereas Phase II uses infinite series expansions, that are slightly more complex, to convert the Phase I data set into the final TimeWave. The formalization and comparison work described in this report is concerned only with the Phase I mathematics.

Until recently, the details of the genesis and development of *Novelty Theory* and the TimeWave, although available to all with the will and energy to examine them, have remained largely out of sight and out of mind for most. The primary focus has been on the results of that development – i.e. the reflective and apparently projective characteristics of *Novelty Theory* as expressed by the TimeWave, and graphed by the TWZ software. That is, until Mathew Watkins, a British mathematician proceeded to deconstruct the wave generating process and examine those details more closely. The results of his investigation were reported in a paper entitled [Autopsy for a Mathematical Hallucination](#)<sup>3</sup>, linked to the McKenna website [Hyperborea](#) as the [Watkins Objection](#).

There were several things that Watkins found objectionable in his scathing critique of *Novelty Theory* and TWZ, but there was only one significant finding that he

substantiated in his report. He showed that one of the operational steps used in the production of the 384 number data set, the notorious “half twist”, was not mathematically consistent with the standard linear analysis that is implied by the documentation in *the Invisible Landscape* and the *Time Explorer* software manual. He pointed out the fact that the two number sets produced by first the inclusion, then the exclusion of the half twist would be different sets resulting in different *TimeWaves*. However, he didn’t quantify this difference in number sets, nor show what the resulting impact of the final TimeWave would be. He then concluded that without some miraculous justification for the “half twist”, his findings would prove fatal to *TimeWave Zero* and *Novelty Theory*. This claim seemed somewhat speculative and overstated to me, since he hadn’t actually shown what the impact of his findings on the *TimeWave* itself would be. Nonetheless, it was an important finding, so I decided to investigate the matter for myself in order to assess the actual impact on the *TimeWave* and the corresponding damage to *Novelty Theory*. This meant, of course, that I would have to immerse myself in the details of the TWZ mathematical development.

Becoming familiar with the details of the mathematical development of TWZ proved to be more of a challenge than expected, partially because the available documentation lacked the necessary descriptive detail to faithfully reconstruct the process of TimeWave generation. Additionally, some of the mathematical operations were described with unconventional language that was somewhat confusing, making it more difficult to understand what was actually being done. So in order to clarify this process of wave generation, I proceeded to delineate and mathematically formalize each of the steps in the process that takes one from the King Wen hexagram sequence to the final 384 number data set - Phase I of the TimeWave generating process. I felt that it was important as well, that this formalization be done in a way that could be clearly visualized, in order to give one a mental picture of what might actually be happening as one proceeds through the development process. I felt that it should be more than merely a correct, but arcane, mathematical formulation.

An important feature of the standard development process, clearly shown in all the *TimeWave Zero* documentation, is that the process is expressed by piecewise linear mathematics – meaning simply that the final 384 number data set is the result of the expansion and combination of straight line segments. These linear segments are bounded by integers that are derived from the FOD number set, although the actual inclusion of the line segments establishes non-integer values in the set. Another important and well-documented feature of the process, is the generation of the simple bi-directional wave from the FOD number set. This bi-directional wave consists of a forward and reverse flowing wave pair, and it is the fundamental waveform or building block of the *TimeWave* generating process. These two features, a piecewise linear nature and wave directed flow, clearly lend themselves to expression through the principles of vector mathematics. Vector notation and operations were consequently chosen as appropriate tools for this modeling process.

It should be noted here, that there is nothing unique or exceptional about the use of vector mathematics. It is only one of several approaches that could have been used; but it is one that clearly expresses the notion of wave directed flow, and one that also has the capacity to generate straight-line segments. The fact is that only a few of the basic

features of vectors are used here – vector addition and subtraction, and the vector parametric equation of the straight line. However, the generation of straight-line segments using vectors, converts the discrete function (integer values only) represented by the FOD number set, into a continuous function in the domain bounded by the FOD integers. This is important if the wave is to be well defined over the entire range of its expression (i.e. the inclusion of fractional values).

This work is the formalization of the procedures already established with the standard wave development, by McKenna, but one that removes inconsistencies and makes the process more coherent and intelligible. It does not, in any way, make fundamental changes in the development process, nor does it modify the underlying theory.

## Generating the Simple Bi-directional Wave

### (1) The Simple Forward Wave

The process by which the 384 number data set is generated begins with the King Wen sequence of I-Ching hexagrams (a listing of which appears in the *Time Explorer*© manual, pp. 58-59), which is believed to be the earliest arrangement of hexagrams. McKenna chose to examine<sup>4</sup> the number of lines that change (yin to yang, and yang to yin) as one moves from hexagram to hexagram, beginning at hexagram 1 and proceeding to hexagram 64, and he called this quantity the *First Order of Difference* (FOD). The FOD number set that is generated as one moves from hexagram 1 to hexagram 64 contains 63 elements; a 64<sup>th</sup> element is determined by recording the FOD as one moves from hexagram 64 “wrapping” back to hexagram 1, thus establishing a closed system with periodic waveform. This FOD number set can be computed mathematically by treating each hexagram as a binary number as reported by Meyer<sup>5</sup>, but in this case I simply recorded each number manually in *DeltaGraph*®<sup>6</sup> and *Excel*®<sup>7</sup> spreadsheets.

The FOD number set, which I will now call the *Simple Forward Wave*<sup>8</sup>, is graphed in Fig. 1 with straight line segments connecting the individual FOD data points. The  $x$ -axis of this graph shows the hexagram transition number, where transition  $n$  is defined as the transition from hexagram  $n$  to hexagram  $n+1$ ; transition  $n=0$  is simply an  $x$ -axis wrap of transition 64, and is thus defined as the transition from hexagram 64 to hexagram 1. The inclusion of the zero transition data point is a way of graphically illustrating the “wrap-around” nature of this number set, or possibly a way of mapping an apparent 3-dimensional cylindrical surface onto a 2-dimensional plane. For clarity, let us define this feature of the FOD number set:

#### Definition 1:

The collection of simple forward wave  $x, y$  integer pairs, or FOD number set  $[X_n, Y_n]$ , form a closed loop such that the final value  $[64, Y(64)]$  “wraps” to an initial value  $[0, Y(0)]$ ; Where  $Y(64) = Y(0)$ , and the waveform is periodic.

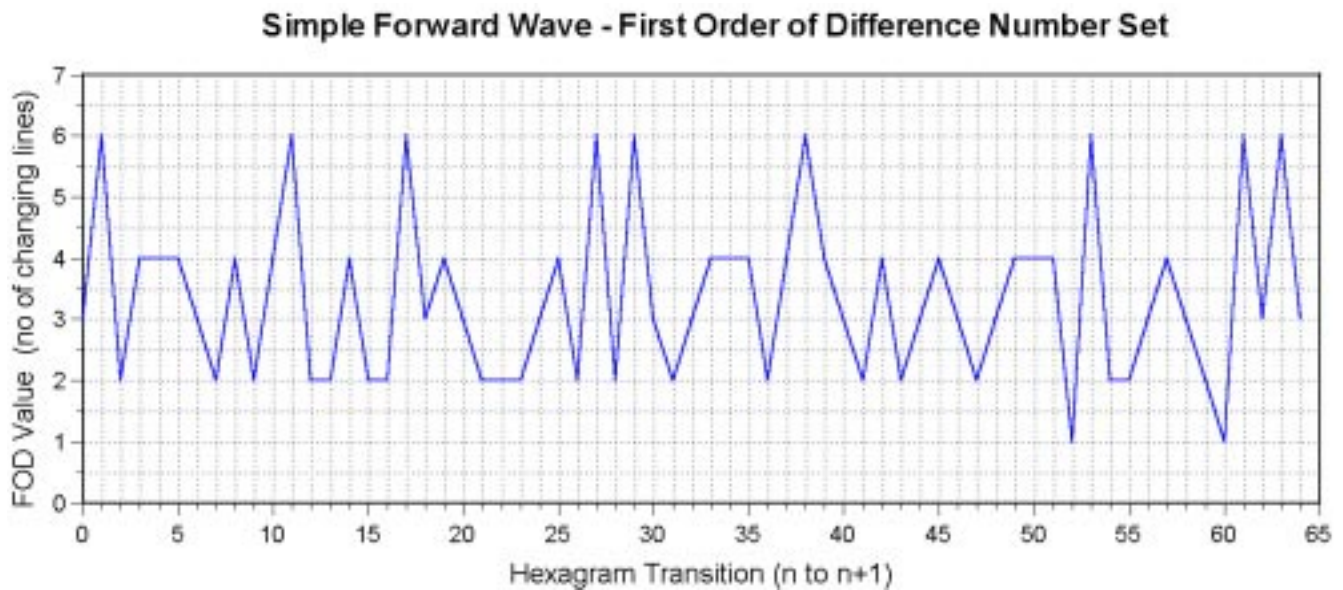
The  $y$ -axis values shown in Fig. 1 are the actual FOD transition values, integers that would normally be shown as points along the transition axis. In Fig. 1, however, these points are connected by straight line segments, which establishes the piecewise linear

nature of this number set, generating non-integer values and creating a general *function* that is defined at every point in its domain (all possible  $x$  values in the domain  $0 \leq x \leq 384$ ). Generating this function requires the acceptance of a general principle, which will now be defined for clarity:

**Definition 2:**

The collection of FOD numbers is a set of integers that establish the boundary conditions for a piecewise linear *function*, which is defined for all  $x$  in the domain of the FOD set and its expansions. The domain of  $x$  is defined:  $0 \leq x \leq 384$

This FOD *function* is viewed as having a forward flowing, or  $+x$  directed nature, and it is the basic or simplest number set in the TimeWave development process. Thus it is called the simple forward flowing wave, or just the *Simple Forward Wave*.



**Figure 1**

**(2) [The Simple Reverse Wave](#)**

In order to clarify the process of simple bi-directional wave generation, and the production of the *Simple Reverse Wave*, let us first define another general principle:

**Definition 3:**

The Simple Forward Wave (the FOD *function*) has a Reverse Wave partner, and the two are aligned with one another such that closures (nodes) occur at either end of the properly superimposed wave pair. The proper superimposition produces forward and reverse wave closure at the Index 1, and at Indices 62, 63, and 64 endpoints.

This is an important statement, for without it there is neither reason nor unambiguous path for the construction of the bi-directional wave function, nor is the proper form of



wave closure obvious. Once this principle has been established, however, it is then possible to proceed with a step-by-step process of reverse wave, and bi-directional wave generation. Figures 2a–2f illustrate this process of generating the *Simple Reverse Wave*, followed by a closure with the *Simple Forward Wave* to form the *Simple Bi-directional Wave*. Fig. 2a shows Step 1 in the process of *Simple Reverse Wave* generation – a 180° rotation of the Simple Forward Wave about the  $x, y$  axes origin (0,0).

This rotation operation can be visualized by observing that the *Simple Forward Wave*, shown in quadrant I (upper right hand corner of Fig. 2a) is fixed relative to the  $x, y$  axes (red lines). The axes are then spun counter-clockwise 180° around their origin (intersection point), carrying the wave with them. The mathematical formulas for this rotation are expressed as:

$$x' = x \cos \theta + y \sin \theta \quad [1]$$

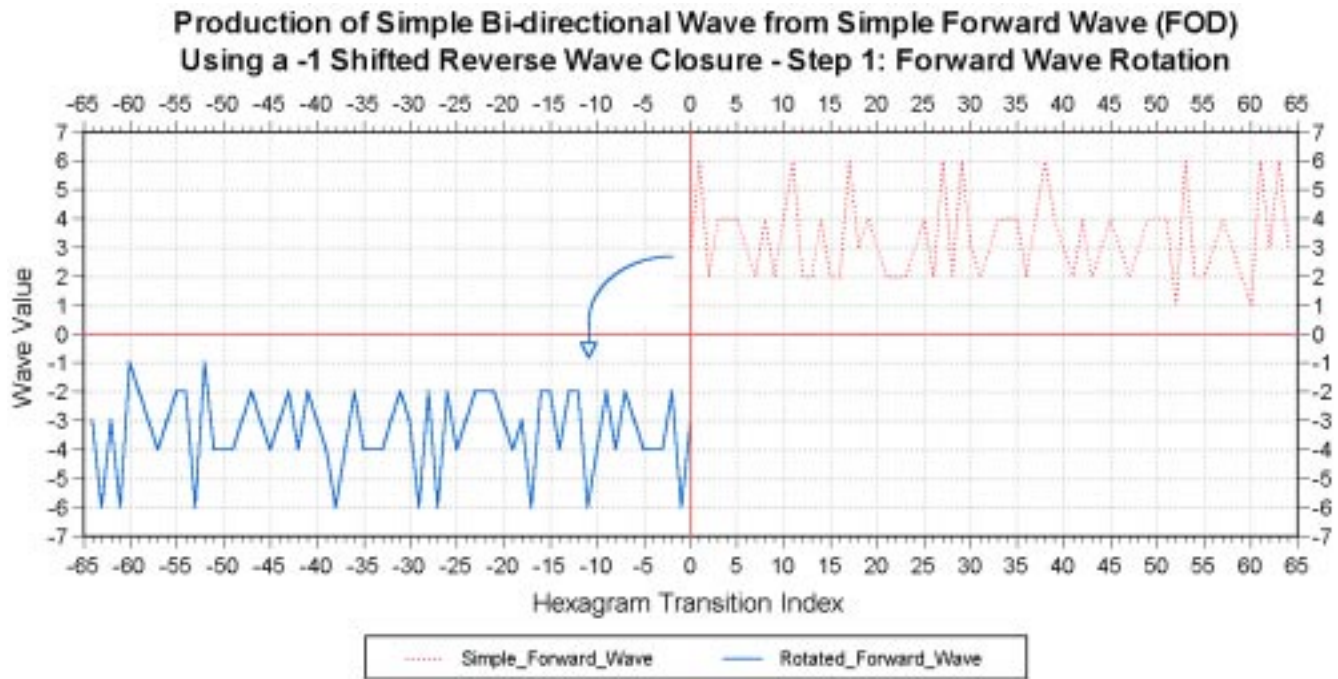
$$y' = -x \sin \theta + y \cos \theta \quad [2]$$

Where:  $x'$  is the rotated  $x$  value  
 $y'$  is the rotated  $y$  value  
 $\theta$  Is the angle of rotation in degrees

With 180° as the rotation angle, these equations reduce to:

$$x' = -x + 0 = -x \quad [3]$$

$$y' = -0 - y = -y \quad [4]$$



**Figure 2a**

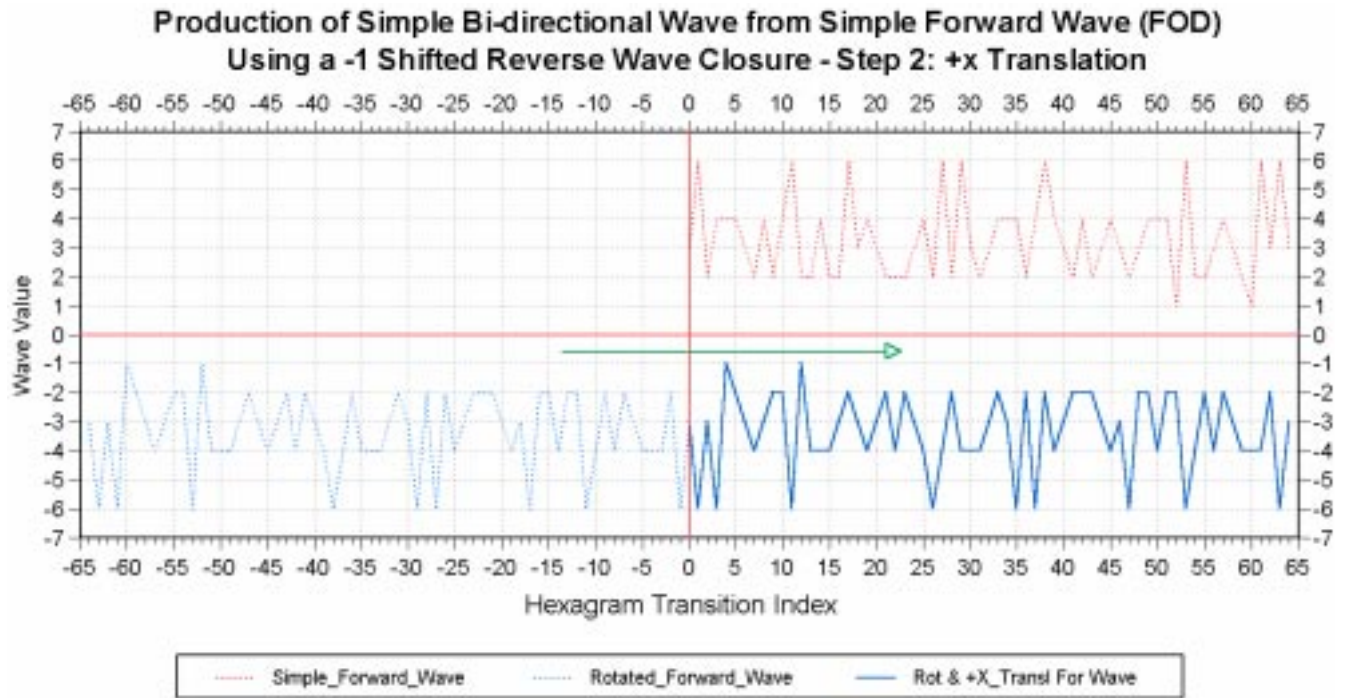
Equation [3] and [4] show that this 180° rotation operation results in a simple sign change of the original forward wave  $x, y$  pair data set. The rotation places the developing reverse wave in quadrant III of the graph, shown as the solid blue line-plot. The dotted blue line-plot shows the position of the parent *Simple Forward Wave*.

Step 2 of the reverse wave generation process is shown in Fig. 2b, and involves the translation of the rotated forward wave in the  $+x$  direction. This operation is expressed by the following translation equation:

$$x = x' + h \quad [5]$$

Where:  $x$  is the translated value of  $x'$  of equation [3]  
 $h$  is the magnitude of the translation in the  $+x$  direction

Since this translation must  $x$ -align the endpoints of the forward and reverse waves, the magnitude of the translation,  $h$ , is +64. This positions the developing reverse wave in quadrant IV as shown in Fig. 2b.



**Figure 2b**

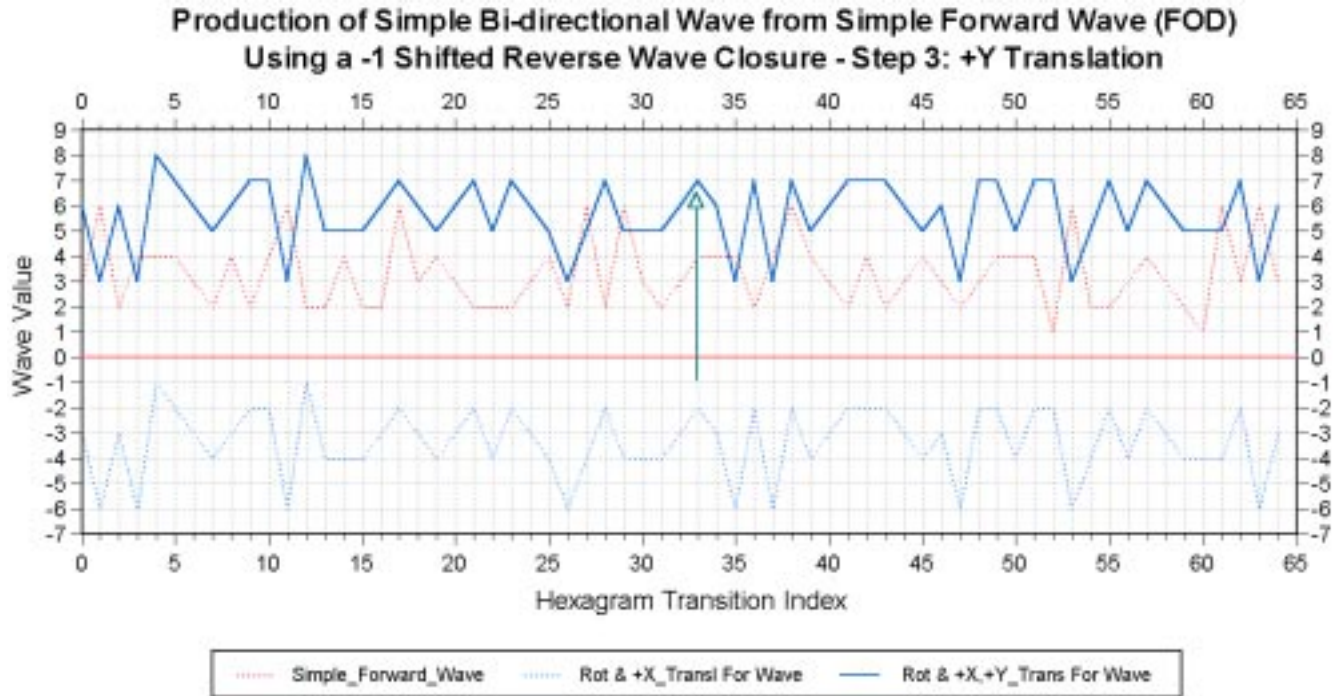
Fig. 2c shows Step 3 of the reverse wave generation process, and is defined as the  $+y$  translation of the  $x$ -translated wave of Fig. 2b. This translation is performed so that the forward and reverse waves will be in position to achieve closure at the Index 1 and Indices 62, 63, 64 endpoints as specified by definition 3, once the next and final step is performed. The translation equation for this step of the process is express as follows:

$$y = y' + k \quad [6]$$

Where:  $y$  is the translated value of  $y'$  as expressed in equation [4]  
 $k$  is the magnitude of the translation required to position the reverse wave for proper closure with the forward wave

In this case the  $y$  positioning for proper wave closure requires a  $k$  value of +9. Fig. 2c shows the reverse wave position that results from this translation, and also shows that the forward and reverse waves are offset, and have not yet achieved endpoint closure. The next and final step is performed using a different type of mathematical operation called the “shift”, which can be understood by using the following analogue:

Take 65 marbles and place them in the slots of a roulette wheel that has been “unrolled”, so that the slots are in a straight line rather than a circle. The slots are numbered from 0 to 64, and each marble is placed contiguously in its designated slot. Now remove marble #0 from its slot, and shift marble #1 to its place, then continue the process up the line until all the remaining marbles have been shifted down one slot. Now place the marble from slot #0 into slot number 64 and you have a  $-1$  shifted marble train. This is the type of shift that is necessary to achieve forward and reverse wave closure at the Index 1 and Index 64 endpoints, shown in the next figure, by using line segments instead of marbles.



**Figure 2c**

This final step, the  $-1$   $x$ -shift, is shown in Fig 2d, where the dotted blue line-plot is the pre-shifted reverse wave position, and the solid blue line-plot is the  $-1$   $x$ -shifted reverse wave position. The larger plot at the top shows the shift operation for the overall wave



pair, whereas the two smaller plots at the bottom of Fig. 2d are magnifications showing the closure process at the beginning and end sections of the wave pair. The mathematics for this operation can be expressed as a two step process as follows:

$$\text{For } 0 \leq x \leq 64 \quad f(x_s) = f(x+1) \quad [7]$$

$$\text{Where } f(65) \text{ is defined: } f(65) = f(0) \quad [8]$$

such that:  $f(x_s)$  is the  $y$  value of the  $-1$   $x$ -shifted wave at  $x$

and:  $f(x+1)$  is the  $y$  value of the pre-shifted reverse wave at  $x+1$

There are two features of Fig. 2d that should be noted here. First notice that in the small graphs at the bottom, closure between the forward and reverse waves occurs at four transition axis points (excluding zero). These points are  $x = 1$ ,  $x = 62$ ,  $x = 63$ , and  $x = 64$ , so that wave closure occurs at one initial point ( $x = 1$ ) and three terminal points. Point zero is excluded since it is simply a “wrap”, or duplicate, of point 64 and will eventually be discarded. Secondly, the two smaller graphs at the bottom of Fig. 2d show the process of endpoint shift, or transferring the “marble/line segment” that was initially in slot 0 into the vacated end slot 64. The green arrow line runs from line segment 1 in the graph at the left, to line segment 64 in the graph at the right, and shows that segment 1 is being transferred to segment 64 as the  $-1$   $x$ -shift is performed. The figure shows that this is not a simple translation operation as in the previous two steps, but a definite shift – much like the operation of a shift register in digital electronics. Note that if a simple  $-x$  translation were performed, line segment 1 would be translated into the negative  $x$  domain to the left of the  $y$ -axis, and there would be no line segment 64.

With the performance of the  $-1$   $x$ -shift operation, the production of the *Simple Bi-directional Wave* is now complete. We have thus created a forward and reverse flowing waveform, which is closed at either end, something like nodes on a standing wave. Although this is the correct procedural process for generating the reverse wave from the forward wave, and for producing endpoint closure, the relationship between forward and reverse waves can be expressed simply by the following equations:

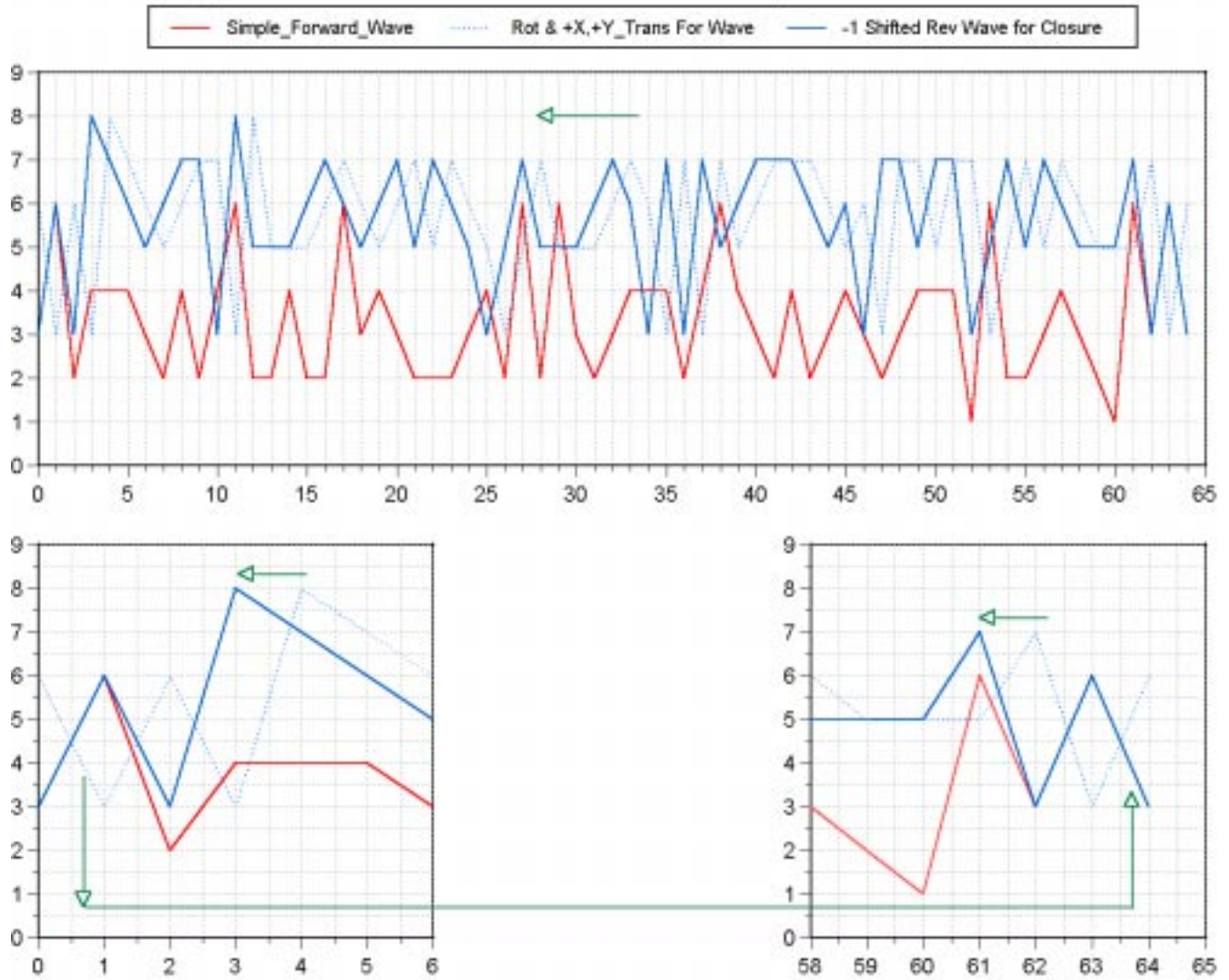
$$\text{For } 0 \leq x \leq 64 \quad f(x_r) = 9 - f(63 - x) \quad [9]$$

$$\text{Where } f(-1) \text{ is defined: } f(-1) = f(64) \quad [10]$$

and where:  $f(x_r)$  is the  $y$  value of the reverse wave at  $x$

$f(63 - x)$  is the  $y$  value of the forward wave at  $(63 - x)$

## Production of Simple Bi-directional Wave from Simple Forward Wave (FOD) Using a -1 Shifted Reverse Wave Closure - Step 4: Reverse Wave Shift



**Figure 2d**

Equations [9] and [10] are good examples of mathematics that do the job, but fail to give one a visual image or sense of what is really going on in the process. This type of math is actually quite useful, nonetheless, for computer generation of the reverse wave number set.

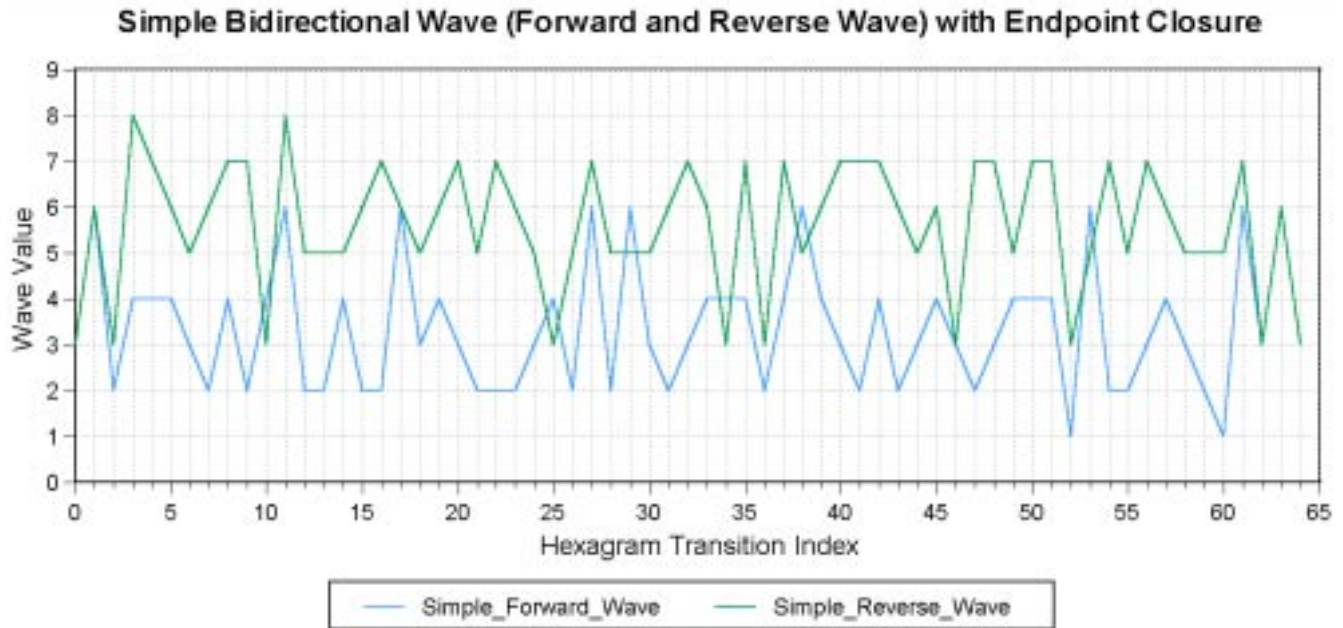
We have thus created a simple bi-directional waveform, having the properties of directed flow and endpoint closure, and which can be characterized as a piecewise linear function – a function we have yet to define over its non-integer domain. That will be our next step in the formalized development of the *TimeWave data set*.

### [Vector Expression of the Piecewise Linear Function](#)

The *Simple Bi-directional Wave*, as described thus far, is fundamentally a collection of

$[x, y]$  integer data points, that are generated by the FOD number set and the performance of several subsequent mathematical operations. By connecting these points with straight line segments we are inferring that some piecewise linear process is responsible for filling in the gaps between integers, creating a continuous function over the domain defined by these endpoint integers. However, we have yet to define such a function mathematically - a necessary process if we are to correctly expand the *Simple Bi-directional Wave* into the *Tri-Level Complex Wave*, or 384 number data set.

Fig. 3 shows the *Simple Bi-directional Wave* in its final form. The forward and reverse waves are properly superimposed with the correct endpoint closure, and the data set integers are connected with straight-line segments. Note that the primary closures occur at transition index 1 and index 62, with secondary closures and index 63 and 64. A primary endpoint closure, in this context, is simply the first endpoint closure point as seen from *within* the bi-directional wave envelope (area enclosed by the double waveform), whereas a secondary endpoint closure point would be all subsequent points of closure. The notion of primary and secondary wave closure is introduced here because it will be used later when the *trigramatic* and *hexagramatic* waves are generated and then indexed with the linear wave.



**Figure 3**

Although Fig. 3 shows the properly superimposed forward and reverse waves, there is nothing in the graph that provides this sense of directed flow, except the wave labeling. Fig. 4 introduces, for the first time, vector representation of the forward and reverse wave segments, providing a visual image of wave directed flow. This graph shows the forward and reverse waves engaged a continuously flowing process – forward wave flows into the reverse wave, and the reverse wave flows back into the forward wave. This dynamic and continuous cycle is akin to the flow from Yin to Yang, Yang to Yin, expressed in the well-known Yin-Yang symbol. It is also similar to a process that is described in quantum theory, as the flow of matter to energy, energy to matter, in a

continuous and never-ending cycle. Fig. 4 can be then viewed as a continuously flowing counter-clockwise loop – always in motion, and always changing. So how is this process to be expressed mathematically so that these principles are preserved, and so they might be expanded into a form of higher ordered expression? This is where the principles of vector mathematics can serve the process well.

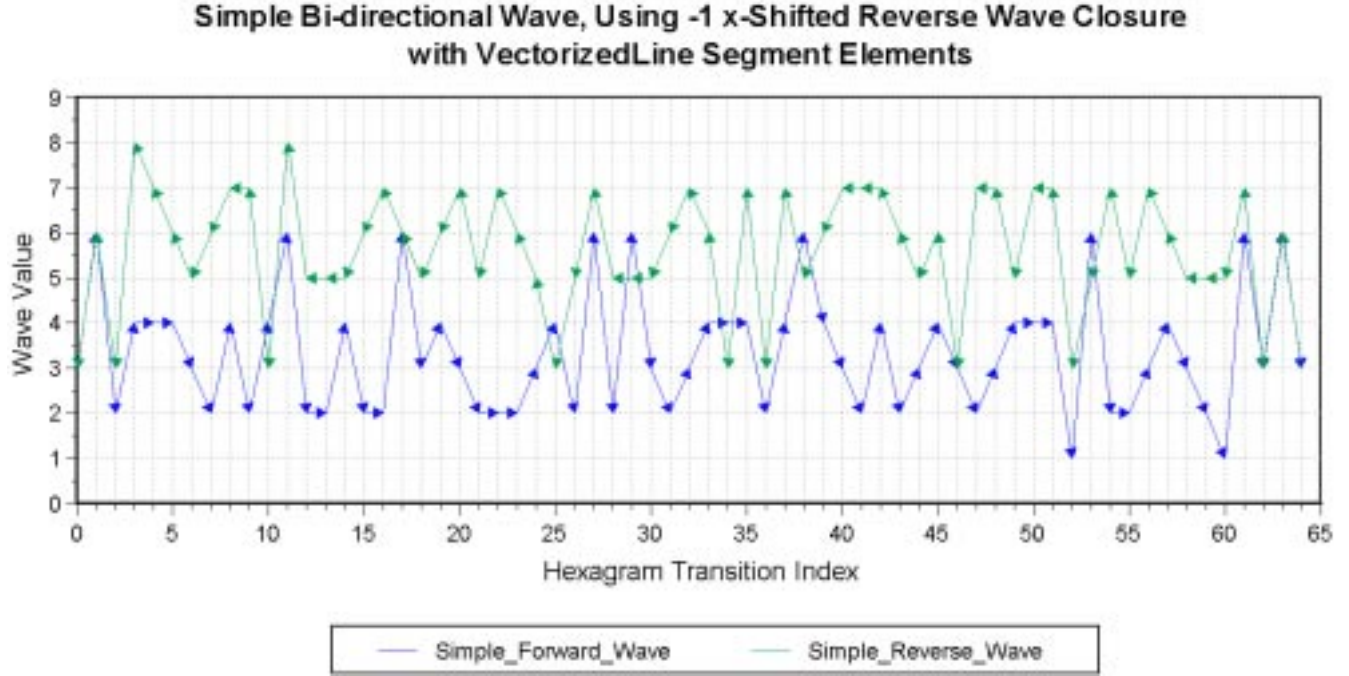


Figure 4

The graph in Fig. 5 shows the generalized form of forward and reverse wave linear elements, expressed as vectors  $\vec{F}_{1(i)}$  for the forward wave segment, and  $\boxed{\times}$  for the reverse wave segment. The subscript 1 in this vector notation signifies that this vector is a first order element (i.e. a *linear* wave element as opposed to a *trigramatic* or *hexagramatic* element), and the  $\boxed{\times}$  subscript signifies that this segment is the  $i$ -th element of the forward and reverse wave line segment set. The vectors  $\mathbf{0A}$ ,  $\mathbf{0B}$ ,  $\mathbf{0C}$ , and  $\mathbf{0D}$  are construction vectors for  $\boxed{\times}$  and  $\boxed{\times}$ , whereas vectors  $\mathbf{0P}$  and  $\mathbf{0Q}$  are variable, or parametric vectors that map the lines along which  $\boxed{\times}$  and  $\boxed{\times}$  lie.

In this graph, the x-axis values correspond to the FOD transitions, with  $\boxed{\times}$  or  $\boxed{\times}$  being the  $i$ -th FOD transition, and  $\boxed{\times}$  or  $\boxed{\times}$  being the  $i$ -th +1 transition, and together they define the domain of the linear bi-directional wave elements. The y-axis values in Fig. 5 correspond to the magnitude of the forward and reverse waves, with  $\boxed{\times}$  and  $\boxed{\times}$  being the  $i$ -th integer values (at  $x = i$ ) of the forward and reverse waves respectively. The values  $\boxed{\times}$  and  $\boxed{\times}$  are the  $i$ -th +1 integer values (at  $x = i+1$ ) of the forward and reverse waves respectively. These y values define the range of the *Simple Bi-directional Wave*, from the forward and reverse wave values:  $\boxed{\times}$ . The subscript  $i$  is important



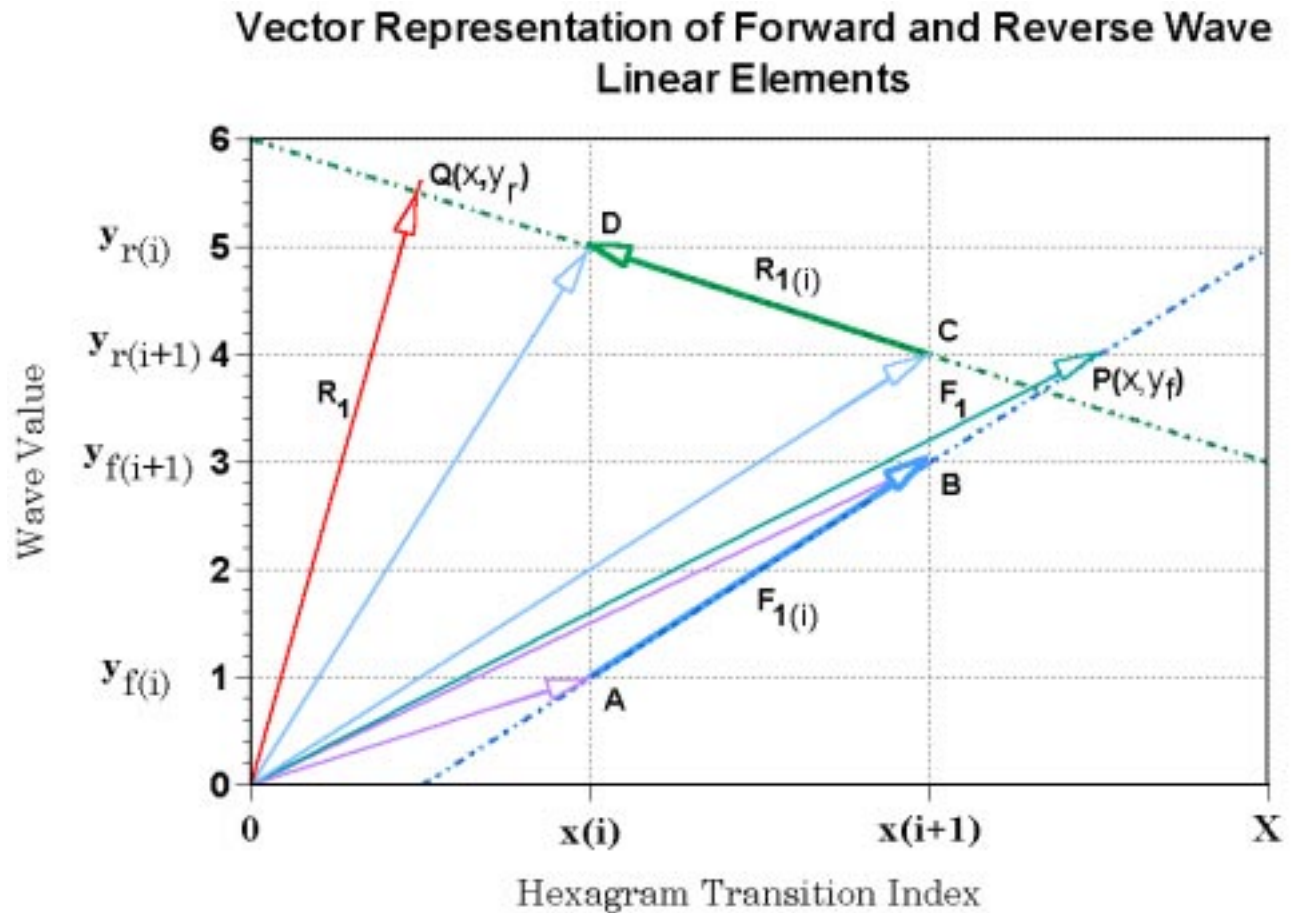
here because it establishes the boundary conditions (x domain) within which each line segment expresses itself. This subscript is associated with the *linear wave*, and is a function of the independent variable  $x$ . Let us define  $X = \{x\}$  as the set of all positive real numbers in the domain of the TWZ *data set*, ✖ and the subscript  $i$  as a function of  $x$ :

$$\text{int}\left(\frac{x}{\Delta x}\right)$$

[11]

Where  $\text{int}()$  indicates the argument  $x$  is rounded down to its integer value.

The vector notation view of Fig. 5, can be viewed as an abstraction for motion or flow. With this notation we leave the realm of classical geometry, or statics, and enter the realm of kinematics – the path of a moving point. When sketching a line or a curve with pencil, for example, the point of the pencil occupies a unique position on the line or curve





**Figure 5**


at any given instant of time. Then as we move our hand, the position of the pencil point changes in time and traces the line or curve. This is essentially how vector mathematics serves the foundation and spirit of the 384 number data set development. Similarly, the *Simple Bi-directional Wave* describes the path of a moving point, a counter-clockwise



flow of some entity, be it matter, energy, photon, graviton, *novelton*, or *eschaton*. In this dynamic or kinematics process, we will make use of the notion of the *parameter*.

The *parameter* has been described by Anderson<sup>9</sup> as *an independent variable which serves to determine the coordinates of a point or describe its motion*. This is the notion that will be used here, to establish the vector parametric equation of the straight line in a plane. Again, according to Anderson<sup>9</sup> the *parametric form tells us where the point goes, when it gets there as well as the curve along which it travels*. Before this parameterization is begun, however, vectors  and  must first be defined mathematically.

### (1) [Forward Wave Vector Equations](#)

Referring to Fig. 5, the forward wave vector , for the *i*-th transition element can be expressed as directed line segment **AB**:

$$\boxed{\text{red X}} \quad [12]$$

and the vector **0B** is expressed:

$$\boxed{\text{red bowtie}} \quad [13]$$

Rearranging equation [13]:

$$\boxed{\text{red bowtie}} \quad [14]$$


Substituting standard form:

$$\boxed{\text{red bowtie}} \quad [15]$$

Which reduces to:

$$\boxed{\text{red bowtie}} \quad [16]$$

### (2) [Reverse Wave Vector Equations](#)

The reverse wave vector , for the *i*-th transition element can be expressed as directed line segment **CD**:

$$\boxed{\text{red X}} \quad [17]$$

and the vector **0D** is expressed:

$$\boxed{\text{red bowtie}} \quad [18]$$

Rearranging equation [18]:

$$\boxed{\text{red bowtie}} \quad [19]$$

Substituting standard form:

$$\boxed{\text{red bowtie}} \quad [20]$$

Which reduces to:

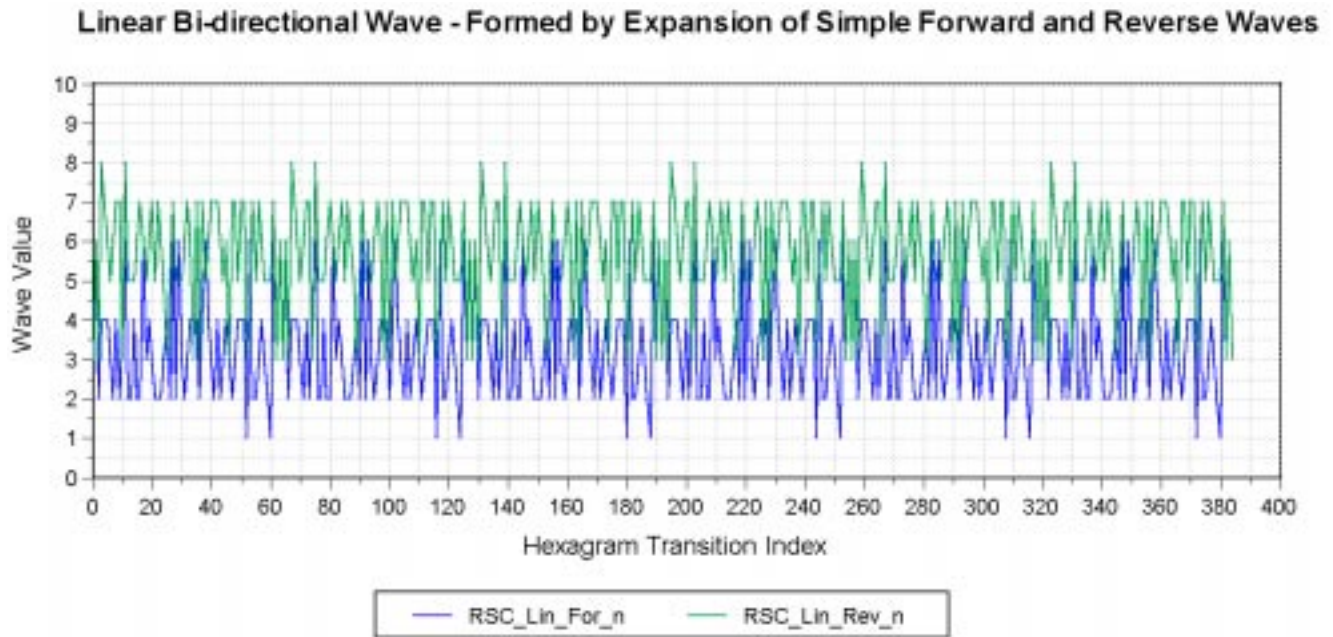
$$\boxed{\text{red bowtie}} \quad [21]$$

With the derivation of equation [16] and [21], we have now defined the generalized forward and reverse wave vectors mathematically. These vector definitions will be used

to formulate the vector parametric equations of the generalized line segment, the basis for the *Simple Bi-directional Wave* and the wave expansions that follow.

### (3) [The Linear Bi-directional Wave](#)

The *Simple Bi-directional Wave* is all that we have thus far defined or described; but this wave forms the basis for the *Linear*, *Trigramatic*, and *Hexagramatic* waves which are all products of the expansion of this basic building block. The first step in the process of wave expansion and combination that eventually leads to the 384 number data set is the generation of the *Linear Bi-directional Wave*. This wave is produced from the *Simple Bi-directional Wave* (SBW) by simple concatenation – i.e. inserting five copies of the SBW end-to-end with the original, and producing six SBW cycles. According to McKenna, the *Linear Wave* is an expression of the six lines that define each I-Ching hexagram - The SBW then represents one line of the hexagram, and there are six SBW connected end-to-end to form the *Linear Bi-directional Wave* (LBW). Fig. 6 is a graph of this expanded SBW, or *Linear Bi-directional Wave* (LBW), and shows the concatenation process that expands the SBW (64 values, excluding zero) into the LBW (384 values, excluding zero). Although this graph does not show the vector structure of Fig. 4 (to avoid crowding the graph), it is implied here. The LBW therefore expresses the same process of directed flow as does the SBW, a counter-clockwise flow of some point entity along the path traced by the forward and reverse waves in Fig. 6.



**Figure 6**

The concatenation process that produces the LBW can be expressed mathematically as follows:

For:



[22]

and for:  $\boxed{\times}$   $\boxed{\times}$  [23]

Where:  $\boxed{\times}$  (pronounced lin of  $i$ ) is the value of the forward or reverse linear wave at transition point  $i$  or at  $\boxed{\times}$ ; and  $\boxed{\times}$  is the value of the forward or reverse linear wave at  $\boxed{\times}$ , where  $\boxed{\times}$  is the remainder when  $i$  is divided by 64.

The *Linear Bi-directional Wave (LBW)* will now be expressed mathematically, and expanded into the *Trigramatic Bi-directional Wave (TBW)*, and *Hexagramatic Bi-directional Wave (HBW)*, using mathematics derived from the vector parametric equation of the straight line.

## Vector Parametric Equations of the Forward and Reverse Line Segments

### (1) The Linear Forward Wave Vector

The *parameter* is introduced by defining the straight line in terms of a point  $\boxed{\times}$ , a vector  $\boxed{\times}$ , and a parameter  $t$ . Refer to Fig. 5 and locate the vectors  $\mathbf{0A}$ ,  $\mathbf{AB}$ , and  $\mathbf{0P}$ . We have already defined vector  $\mathbf{AB}$  in equation [12] as the forward wave vector  $\boxed{\times}$  (Eqn [16]), which establishes a direction for our line segment. Vector  $\mathbf{0A}$  is in standard position (tail positioned at the coordinate system origin), so that it is defined by the position of its head at point  $\boxed{\times}$ . Vector  $\mathbf{0P}$  is the variable or moving vector and, like the moving pencil point, its head traces the path of the straight line that we are interested in. Let us rename vector  $\mathbf{0P}$  as the linear forward wave vector  $\boxed{\times}$ , and since it is in standard position (tail at the origin so that it is defined by the coordinates of its head), it is described mathematically by the following expression:

$$\boxed{\times} \quad [24]$$

in which  $\boxed{\times}$  are the variable coordinates of the vector head. This vector can also be expressed as the sum of vectors  $\mathbf{0A}$  and the forward wave vector  $\boxed{\times}$  as follows:

$$\boxed{\times} \quad [25]$$

Vector  $\mathbf{0A}$  in standard position is expressed as  $\boxed{\times}$

and from equation [16]  $\boxed{\times}$

so that equation [25] can now be expressed as:

$$\boxed{\text{[redacted]}} \quad [26]$$

with the parameter  $t$  having a range:  $\boxed{\text{[redacted]}}$  over the  $x$  domain  $\boxed{\text{[redacted]}}$

Equation [26] can now be solved for  $x$  and  $y_F$ , the general coordinates of the vector  $\boxed{\text{[redacted]}}$ , to determine the *parametric equation of the line* describing the motion of the forward wave. Solving for  $x$  and  $y_F$  yields the following *parametric equations* of the line:

$$\boxed{\text{[redacted]}} \quad [27]$$

$$\boxed{\text{[redacted]}} \quad [28]$$

Solving [27] and [28] for the parameter  $t$  we get:

$$\boxed{\text{[redacted]}} \quad [29]$$

These expressions for the  $x$  and  $y$  variables in equation [29], are the *standard form of the line equation*, and show that the *parameter*  $t$  behaves as an *interpolation operator* for the  $x$  and  $y$  coordinates of the forward wave line segment. Rearranging terms for the variables in equation [29] leads to the *slope y-intercept form* of the straight-line equation, which is a convenient form of expression for the line segment of interest in this development. The *slope y-intercept* form of the line is determined by solving [29] for the variable  $\boxed{\text{[redacted]}}$ , which results in the expression:



$$\boxed{\text{[redacted]}} \quad [30]$$

Define:  $\boxed{\text{[redacted]}}$  and  $\boxed{\text{[redacted]}}$ , so that [29] becomes:





$$\boxed{\text{[redacted]}} \quad [31]$$

which is the *slope y-intercept* form of the forward linear wave line segment, where the slope is  $\boxed{\text{[redacted]}}$ , and the intercept is  $\boxed{\text{[redacted]}}$ . Equation [31] is the vector-derived expression that is used to generate the linear forward wave over the domain  $\boxed{\text{[redacted]}}$ . This forward wave vector generation process is now repeated for the reverse wave vector.


## (2) [The Linear Reverse Wave Vector](#)

The process for generating the *vector parametric equations* for the reverse wave segment is the same as for the forward segment, but with a vector that has the opposite sense (opposite flow) of the forward wave vector. Again, refer to Fig. 5 and find vectors  $\mathbf{0C}$ ,  $\mathbf{CD}$ , and  $\mathbf{0Q}$ . Vector  $\mathbf{CD}$  has already been defined in equation [17] as the reverse wave vector, . Vector  $\mathbf{0Q}$ , like vector  $\mathbf{0P}$ , is the moving variable vector (tail is fixed, but head moves and traces the line of interest) which will trace the path of our reverse wave line segment. We now rename  $\mathbf{0Q}$  as the reverse wave-generating vector  and since it is in standard position it can be expressed as:

$$\begin{bmatrix} \text{red X} \end{bmatrix} \quad [32]$$

In which  are the variable coordinates for the head of . Expressing  as the sum of  $\mathbf{0C}$  and the parameter scaled , we have:

$$\begin{bmatrix} \text{red X} \end{bmatrix} \quad [33]$$

Substituting for  $\mathbf{0C}$  and  we have:

$$\begin{bmatrix} \text{red X} \end{bmatrix} \quad [34]$$

Solving for  $x$  and  $y_R$  yields the following *parametric equations* of the line:

$$\begin{bmatrix} \text{red X} \end{bmatrix} \quad [35]$$

$$\begin{bmatrix} \text{red X} \end{bmatrix} \quad [36]$$


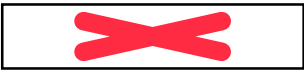

Solving for the parameter  $t$  we get:

$$\begin{bmatrix} \text{red X} \end{bmatrix} \quad [37]$$

then solving for  $y_R$  gives us the *slope y-intercept* form of the linear reverse line segment:

$$\begin{bmatrix} \text{red X} \end{bmatrix} \quad [38]$$



Define:  and , so that [38] is expressed in the slope *y-intercept form* of the linear reverse wave line segment. Notice also that  $\Delta x_{r(i)} = -\Delta x_{f(i)}$ , an identity that will be exploited later. For the *slope y-intercept form* of [38] we substitute the delta () expressions and collect terms:



[39]

Equations [31] and [39] constitute the *defining expressions* for the linear forward and reverse waves respectively, and equation [11] provides the correct value for the subscript *i* in equation [39]. These equations can be either expanded into the trigramatic and hexagramatic bi-directional waves (*TBW* and *HBW*) directly, which are then combined to form complex waves; or they can be first combined into a linear complex wave, then expanded into the trigramatic and hexagramatic complex waves. Either of these two procedures will lead to the same final 384 number data set, but the latter is a more streamlined process that eliminates several operational steps. The complex wave is defined here, as any wave that is a linear combination of one or more bi-directional waves, and is not expressed in bi-directional form. So now let us continue with the process of wave combination, beginning with the linear bi-directional (forward and reverse) wave.

### (3) The Linear Complex Wave

Before beginning the mathematical development of the linear complex wave, let us first establish the procedure for forward and reverse wave combination.


#### Definition 4:

In order to produce forward and reverse wave endpoint (node) closure at zero (0) value, the forward and reverse waves must be subtracted from one another to yield zero valued endpoints for the combined simple wave. In order to maximize the number of positive values for the resultant combined wave, the forward wave is subtracted from the reverse wave.

The linear complex wave is therefore produced by subtracting equation [31] (the forward wave line segment), from equation [39] (the reverse wave line segment). The combined or complex linear wave is thereby expressed as:



[40]

Replacing the expression  with the right hand sides of equation [39] and [31], we get:

$$y_{C1}(x) = \left\{ \left[ \frac{\Delta y_{r(i)}}{\Delta x_{r(i)}} \right] x + \left[ y_{r(i+1)} - \frac{\Delta y_{r(i)}}{\Delta x_{r(i)}} x_{(i+1)} \right] \right\} - \left\{ \left[ \frac{\Delta y_{f(i)}}{\Delta x_{f(i)}} \right] x - \left[ y_{f(i)} - \frac{\Delta y_{f(i)}}{\Delta x_{f(i)}} x_i \right] \right\} \quad [41]$$

and combining like terms and rearranging equation [41] gives us:

$$y_{C1}(x) = \left\{ \left[ \frac{\Delta y_{r(i)}}{\Delta x_{r(i)}} - \frac{\Delta y_{f(i)}}{\Delta x_{f(i)}} \right] x \right\} + \left\{ \left[ y_{r(i+1)} - y_{f(i)} \right] - \left[ \frac{\Delta y_{r(i)}}{\Delta x_{r(i)}} x_{(i+1)} \right] + \left[ \frac{\Delta y_{f(i)}}{\Delta x_{f(i)}} x_i \right] \right\} \quad [42]$$

Using the identity shown previously,  $\Delta x_{r(i)} = -\Delta x_{f(i)}$ , equation [42] is reduced to the *defining equation* for the linear complex wave:

$$y_{C1}(x) = \left\{ - \left[ \frac{\Delta y_{r(i)} + \Delta y_{f(i)}}{\Delta x_{f(i)}} \right] * (x) \right\} + \left\{ \left[ y_{r(i+1)} - y_{f(i)} \right] + \left[ \frac{\Delta y_{r(i)} x_{(i+1)} + \Delta y_{f(i)} x_i}{\Delta x_{f(i)}} \right] \right\} \quad [43]$$

Where  $y_{C1}(x)$  is the *linear complex wave function* and the delta ( $\Delta$ ) functions defined as:

$$\Delta y_{r(i)} = (y_{r(i)} - y_{r(i+1)}),$$

Which is the change in the linear reverse wave dependent variable  $y_r$  over the  $x$  domain of  $x_i \leq x \leq x_{(i+1)}$

$$\Delta y_{f(i)} = (y_{f(i+1)} - y_{f(i)}),$$

Which is the change in the linear forward wave dependent variable  $y_f$  over the  $x$  domain of  $x_i \leq x \leq x_{(i+1)}$

$$\Delta x_{f(i)} = (x_{(i+1)} - x_i),$$

Which is the change in the independent variable  $x$  over the domain of the linear complex wave line segment,  $x_i \leq x \leq x_{(i+1)}$

$$i = \text{int}(x)$$

As defined in equation [11]

Substituting the domain endpoints,  $x_i$  and  $x_{(i+1)}$  for the  $x$ -variable, equation [43] reduces to:

$$@ x = x_i \quad y_{C1}(x) = y_{r(i)} - y_{f(i)} \quad [44]$$

$$@ x = x_{(i+1)} \quad y_{C1}(x) = y_{r(i+1)} - y_{f(i+1)} \quad [45]$$

Which confirms what we observe at the linear wave line segment endpoints, and validates equation [43]

### Expansion of the Linear Complex Wave (LCW)

According to McKenna<sup>10</sup> the Trigramatic wave is an expression of the trigram pair that form each I-Ching hexagram. Since each hexagram has a pair of trigrams, a *Trigramatic Wave* pair is constructed such that the two trigramatic waves are placed end-to-end (concatenated), and have the domain (x-axis range) of six simple wave cycles. The *Trigramatic* wave is also viewed as having a value of three times the linear wave, since a trigram consists of three lines (trigram = 3 x 1 lines). Similarly, the *Hexagramatic* wave is viewed as an expression of the unity of each hexagram, and is constructed so that a single hexagramatic wave occupies the domain of six simple waves cycles (six lines to a hexagram), or two trigramatic wave cycles (two trigrams to a hexagram). Additionally, since the hexagram contains six lines, the hexagramatic wave is seen as six times as large as the simple wave (hexagram = 6 x 1 lines, and hexagramatic wave = 6 x 1 simple waves).

This *Tri-Level Complex Wave* is described as having the same three nested levels of expression as exhibited by an I-Ching hexagram. The top level is the *Hexagramatic Wave*, or hexagram as a whole, which contains the two lower levels, two *Trigramatic Waves* and six *Simple Wave* cycles. The mid level of expression is the *Trigramatic Wave*, which contains the six *Simple Wave* cycles below and is contained by the one hexagramatic cycle above. The bottom level of expression is the *linear wave*, having six simple wave cycles that are contained within two trigramatic wave cycles and one hexagramatic wave cycle.

If we were to look at the complex wave as analogous to some physical wave, be it electromagnetic or acoustic, then this tri-level wave structure could be viewed as harmonic in nature. The hexagramatic wave would then correspond to the wave fundamental or 1<sup>st</sup> harmonic, the trigramatic wave would correspond to the second harmonic (2x the fundamental frequency), and the linear wave would correspond to the sixth harmonic (6x the fundamental frequency). In the case of the *Tri-Level Complex Wave*, however, the harmonic waves are not only frequency multiples, they are also amplitude multiples of the fundamental, or hexagramatic wave. Although this notion of wave harmonics may only be an interesting perspective at this point, it may be useful when examining the wave features of these number sets using Fourier analysis.

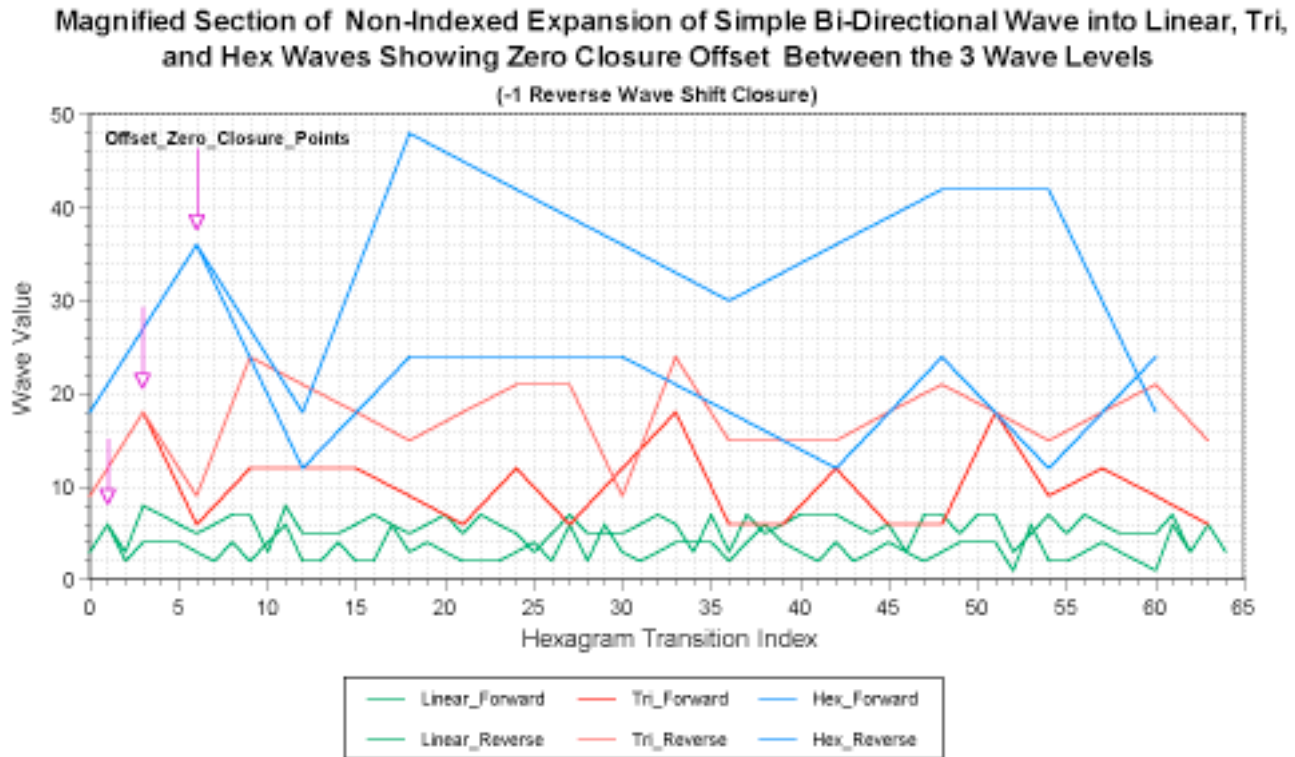
### The Expansion Process Expressed Graphically

Graphically speaking the *Trigramatic Complex Wave* is simply a 3x magnification of the linear complex wave, i.e. the magnification of the first two of its simple wave cycles. This 3x magnification means that the linear complex wave segments are expanded by a factor of three, in both the *x* and *y* directions. Similarly, the *Hexagramatic Complex Wave* is a 6x magnification of the linear complex wave, i.e. the magnification of the first of the

simple wave cycles. Figure 7 is a graphical representation of this process, and shows the 3x and 6x magnification over the first 64 transition index values (64 of 384). The graph shows one complete *linear* cycle, one-third of a *trigramatic* wave cycle, and one-sixth of a *hexagramatic* wave cycle.

One significant feature to notice in Fig. 7, is that *the linear, trigramatic, and hexagramatic* waves are offset from one another – the first peak of each wave level is not aligned with its neighbor. Notice also, that this first peak at each wave level (linear, tri, and hex) occurs at the primary closure point (i.e. the first closure point as observed from within the envelope of the linear, tri, and hex bi-directional waves). For the *linear* wave this closure occurs at index 1, for the *trigramatic* wave it is at index 3, and for the *hexagramatic* wave it occurs at index 6. This is exactly the defining 1-3-6 ratio for *linear, trigramatic, and hexagramatic* waves, which this graph illustrates well.

Another feature to notice about Fig. 7 is that this wave offset is due to the fact that *linear* wave segment 1 is included in the *linear* wave number set. Remember that this first segment (from index 0 to index 1) is a result of the “wrapping” feature of the simple



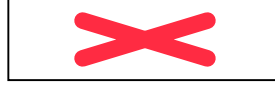
**Figure 7**

Bi-directional wave – transition 64 is wrapped (copied) to transition zero for the simple wave, or transition 384 is wrapped to zero for the entire linear bi-directional wave. Therefore, transition number 0 is not the starting point of the wave, but transition 1 is. Nonetheless, let us mathematically express the linear forward wave expansion, shown in Fig. 7, as follows:



[46]

Or by rearranging terms in [46]:



[47]

Likewise for the linear reverse wave:



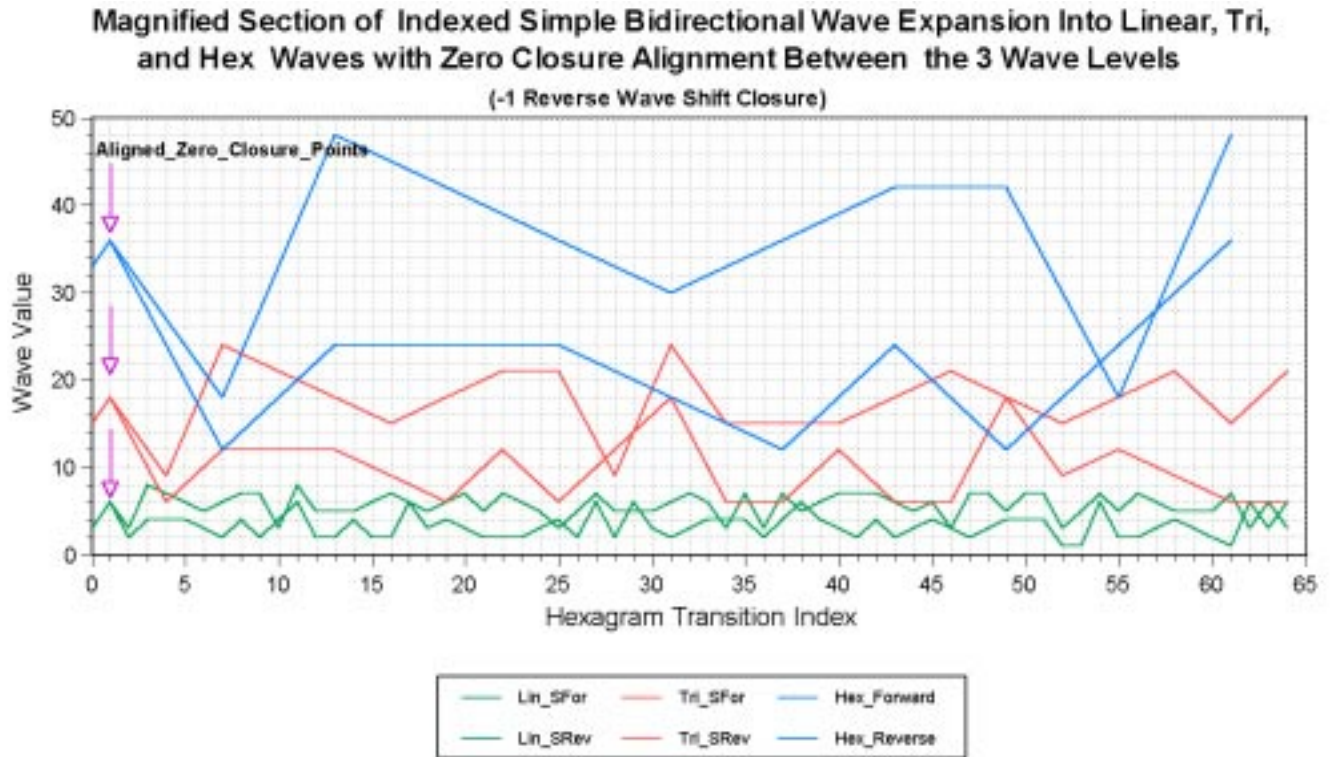
[48]

and rearranging:



[49]

This same set of equations, [46] through [49] can be used to expand the linear wave into the hexagrammatic wave shown in Fig. 7, by replacing all number 3's by 6's. However, since the actual starting point for this wave set is at transition 1 and not transition 0, the proper expansion will look as shown in Fig. 8. In this figure, alignment between linear, trigrammatic, and hexagrammatic waves occurs at transition index 1; also a point of primary closure.



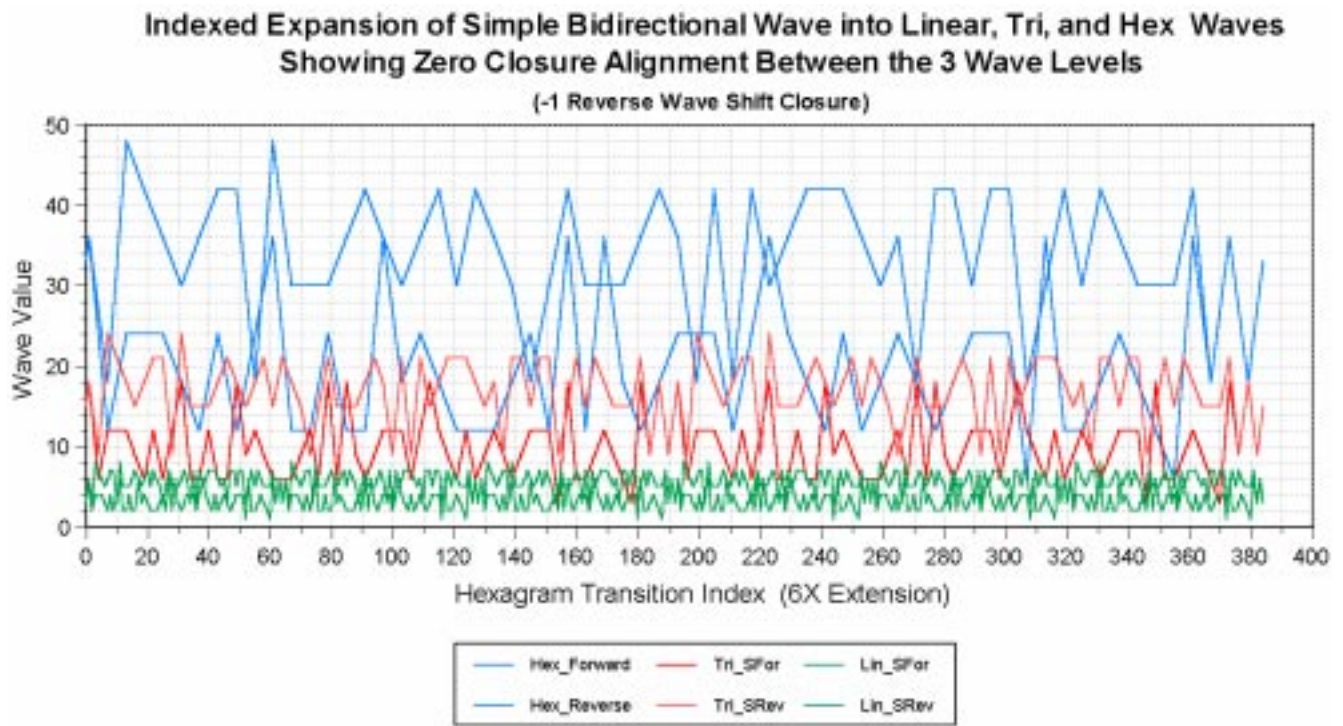
**Figure 8**

Fig. 8 also shows this expansion in terms of the *linear*, *tri*, and *hex* bi-directional waves, in which the linear bi-directional wave is expanded into the *trigrammatic*, and *hexagrammatic* bi-directional waves. However, these bi-directional waves are eventually combined to form the complex wave system, as described by equation [43] for the linear wave case. Since all three bi-directional waves are to be expressed as complex waves,



several operational steps can be omitted and the process streamlined, by expanding the linear complex wave directly. Consequently, we will follow a mathematical process that expands the linear complex wave, described by equation [43], into the tri and hex complex waves. In the interest of maintaining visual clarity of this process, however, and of remaining true to the notion of a directed flowing wave cycle at all three levels of expression, we show the expanded wave system as bi-directional in nature.

Fig. 9 shows the proper expansion of the linear bi-directional wave into the trigramatic and hexagramatic bi-directional waves, with wave indexing at transition 1. This graph shows the entire 384 number wave domain, in which a single *hexagramatic* wave cycle contains two *trigramatic* wave cycles and six linear wave cycles. This notion of all three levels of wave expression being contained, or nested in one level is the actual theoretical basis for the *tri-level wave* combination that produces a single *Tri-Level Complex Wave – the data set*.

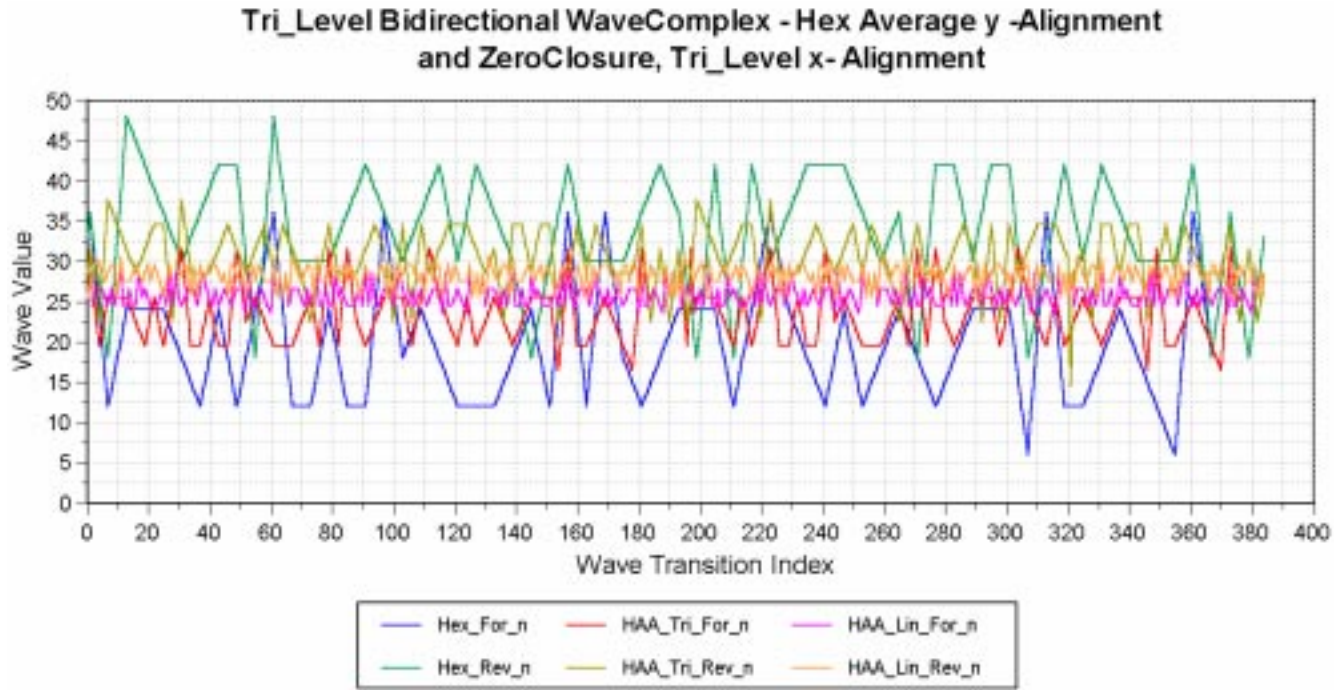


**Figure 9**

Fig. 10 shows the same tri-level bi-directional wave set as Fig. 9, but with the average value of the linear and *trigramatic* bi-directional waves aligned with the average value of the *hexagramatic* wave. These two figures are mathematically equivalent for this development, as we shall see.

Fig. 10 is included here because it is the form of the *Tri-Level Bi-directional Wave* that appears in the TWZ documentation, and it is obvious that it looks different than Fig. 9. The linear and trigramatic bi-directional waves in Fig. 10 have their average values aligned to the hexagramatic wave average value, so that they move about a common line – the hexagramatic average. This graph may look different than Fig. 9, but the fact is that they are identical mathematically. The reason is that, in order to produce the

combined complex wave, the forward wave is subtracted from the reverse wave, as shown in equations [40] through [43]. Since the forward and reverse waves remain



**Figure 10**

closed, or connected at their endpoints, it doesn't matter where along the y-axis they are shifted – the resulting difference is the same. Consequently, Fig. 9 is equivalent to Fig. 10, and the graphs appearing in the TWZ documentation.

So let us now begin with the mathematical expansion of the *Linear Complex Wave*, of equation [43], into the *Trigramatic* and *Hexagramatic Complex Waves*, and then finally into the *Tri-Level Complex Wave* – the 384 number *data set*.

## The Mathematics of the Trigramatic and Hexagramatic Complex Waves

### (1) The Trigramatic Complex Wave

Close inspection of Figs 8 and 9 reveals the relationship between the functions describing the linear, trigramatic, and hexagramatic waves. The relationship between linear and trigramatic forward waves is shown in Figs 8 and 9, and is expressed mathematically as follows:

$$y_{F3}(3x-2) = 3y_{F1}(x) \quad [50]$$

Where the quantity within the parentheses is the argument for  $y()$ , and not a multiplier. Rearranging terms in [50] we get:

$$y_{F3}(x) = 3y_{F1}\left(\frac{x+2}{3}\right) \quad [51]$$

Where  $y_{F3}(x)$  is the value of the *trigramatic forward wave* at  $x$ , and  $3y_{F1}\left(\frac{x+2}{3}\right)$  is three times the value of the *linear forward wave* at  $\left(\frac{x+2}{3}\right)$ . Likewise, the *trigramatic reverse wave* is expressed in terms of the linear reverse wave by the equation:

$$y_{R3}(3x-2) = 3y_{R1}(x) \quad [52]$$

and by rearranging terms we get:

$$y_{R3}(x) = 3y_{R1}\left(\frac{x+2}{3}\right) \quad [53]$$

The trigramatic complex wave is defined in the same manner as the linear complex wave, with the tri forward wave subtracted from the tri reverse wave as in equation [40] and expressed in trigramatic terms by:

$$y_{C3}(x) = y_{R3}(x) - y_{F3}(x) \quad [54]$$

Using [50], [52], and [54] we can express the trigramatic complex wave in terms of the linear complex wave as follows:

$$y_{R3}(3x-2) - y_{F3}(3x-2) = 3y_{R1}(x) - 3y_{F1}(x) \quad [55]$$

$$\text{or equivalently:} \quad y_{C3}(3x-2) = 3y_{R1}(x) - 3y_{F1}(x) \quad [56]$$

$$\text{Factoring the right side of [56] gives:} \quad y_{C3}(3x-2) = 3\{y_{R1}(x) - y_{F1}(x)\} \quad [57]$$

Substituting the expression for the linear complex wave on the right hand side of equation [40], into [57]:

$$y_{C3}(3x-2) = 3[\text{lin}(x)] \quad [58]$$

$$\text{then rearranging [58] we get:} \quad y_{C3}(x) = 3\left[\text{lin}\left(\frac{x+2}{3}\right)\right] \quad [59]$$

Equation [59] shows that the value of the *trigramatic complex wave* at  $x$ , is equal to three times the value of the *linear complex wave* at  $\left[\frac{(x+2)}{3}\right]$ . Replacing the  $x$ -term in the  $\text{lin}(x)$  expression of equation [43] with the expression  $\left[\frac{(x+2)}{3}\right]$ , then substituting into [59] gives us the defining equation of the *trigramatic complex wave* as follows:

$$y_{C3}(x) = 3 \left\{ - \left[ \frac{\Delta y_{r(i)} + \Delta y_{f(i)}}{\Delta x_{f(i)}} \right] * \left[ \frac{x+2}{3} \right] + \left[ \frac{\Delta y_{r(i)} x_{(i+1)} + \Delta y_{f(i)} x_i}{\Delta x_{f(i)}} \right] + (y_{r(i+1)} - y_{f(i)}) \right\} \quad [60]$$

In this expression the subscript  $i$  is expressed as a function of  $x$ , using the process similar to that which produced equation [11]. In this case, since the  $x$  term has become  $[(x+2)/3]$ , the expression defining the bounding subscript  $i$  then becomes:

$$i = \text{int}\{(x+2)/3\} = j \quad [61]$$

Where subscript  $i$  is renamed as  $j$  to distinguish it from the linear wave expression subscript shown in the previous linear wave equations. Equation [61] defines subscript  $j$  as the rounded down integer value of the function  $(x+2)/3$ , thus establishing the boundary conditions for the trigramatic line segment mapped by this function.

Equation [60] expresses the *Trigramatic Complex Wave (TCW)* as an expansion of the *Linear Complex Wave (LCW)* directly. However, the same result would be obtained if the linear forward and reverse waves had been expanded into the trigramatic forward and reverse waves, and those results combined to for the *trigramatic complex wave*. This direct approach clearly eliminates two very detailed mathematical steps. The same series of steps will now be used to find the expression for the *hexagramatic complex wave*.

## (2) The Hexagramatic Complex Wave

As for the trigramatic wave, inspection of Figs. 8 and 9 reveals that the relationship between the linear forward wave and the hexagramatic forward wave can be expressed:

$$y_{F6}(6x-5) = 6y_{F1}(x) \quad [62]$$

Rearranging terms for this function we get:

$$y_{F6}(x) = 6y_{F1}\left(\frac{x+5}{6}\right) \quad [63]$$

Where  $y_{F6}(x)$  is the value of the hexagramatic forward wave at  $x$ , and  $6y_{F1}\{(x+5)/6\}$  is six times the value of the linear forward wave at  $\{(x+5)/6\}$ . Likewise, the hexagramatic reverse wave is expressed in terms of the linear reverse wave by the equation:

$$y_{R6}(6x-5) = 6y_{R1}(x) \quad [64]$$

and by rearranging terms we get:

$$y_{R6}(x) = 6y_{R1}\left(\frac{x+5}{6}\right) \quad [65]$$

The *hexagramatic complex wave* is defined in the same manner as the *linear* and *trigramatic complex waves*, with the hex forward wave subtracted from the hex reverse wave as in equation [40] and [54], and expressed in hexagramatic terms by:

$$y_{C6}(x) = y_{R6}(x) - y_{F6}(x) \quad [66]$$

Using [62], [64], and [66] we can express the *hexagramatic complex wave* in terms of the *linear complex wave* as follows:

$$y_{R6}(6x-5) - y_{F6}(6x-5) = 6y_{R1}(x) - 6y_{F1}(x) \quad [67]$$

or equivalently:  $y_{C6}(6x-5) = 6y_{R1}(x) - 6y_{F1}(x) \quad [68]$

Factoring the right side of [68] gives:  $y_{C6}(6x-5) = 6\{y_{R1}(x) - y_{F1}(x)\} \quad [69]$

Substituting the expression for the linear complex wave on the right hand side of equation [40], into [69]:

$$y_{C6}(6x-5) = 6\{\text{lin}(x)\} \quad [70]$$

then rearranging [70] we get:  $y_{C6}(x) = 6\{\text{lin}(\frac{x+5}{6})\} \quad [71]$

Equation [71] shows that the value of the *hexagramatic complex wave* at  $x$ , is equal to six times the value of the *linear complex wave* at  $\{(x+5)/6\}$ . Replacing the  $x$ -term term in the  $y_{C1}(x)$  expression of equation [43] with the expression  $\{(x+5)/6\}$ , then substituting into [71] gives us the defining equation of the *hexagramatic complex wave* as follows:

$$y_{C6}(x) = 6\left\{-\left[\frac{\Delta y_{r(i)} + \Delta y_{f(i)}}{\Delta x_{f(i)}}\right] * \left[\frac{x+5}{6}\right] + \left[\frac{\Delta y_{r(i)} x_{(i+1)} + \Delta y_{f(i)} x_i}{\Delta x_{f(i)}}\right] + (y_{r(i+1)} - y_{f(i)})\right\} \quad [72]$$

In this expression the subscript  $i$  is expressed as a function of  $x$ , using the process similar to that which produced equations [11] and [61]. In this case, since the  $x$  term has become  $[(x+5)/6]$ , the expression defining the bounding subscript  $i$  then becomes:

$$i = \text{int}\{(x+5)/6\} = k \quad [73]$$

Where subscript  $i$  is renamed as  $k$  to distinguish it from the linear and trigramatic wave expression subscripts shown in the defining wave equations. Equation [73] defines subscript  $k$  as the rounded down integer value of the function  $(x+5)/6$ , thus establishing the boundary conditions for the *hexagramatic* line segment mapped by this function.



As with the *Trigrammatic Complex Wave (TCW)* expressed in [60], equation [72] expresses the *Hexagrammatic Complex Wave (HCW)* as an expansion of the *Linear Complex Wave (LCW)* directly. Similarly, the same result would be obtained if the linear forward and reverse waves had been expanded into the hexagrammatic forward and reverse waves, and those results combined to form the *hexagrammatic complex wave*. With the *linear* [43], *trigrammatic* [60], and *hexagrammatic* [72] *complex waves* now defined mathematically and expressed graphically, we are now in a position to combine them to form the *Tri-Level Complex Wave*, or 384 number “data set”.

### (3) [The Combined Tri-Level Complex Wave](#)

Now that the three levels of *TimeWave* expression have been described and defined mathematically, we are now in a position to integrate these three levels into a single unitary system of expression. The *Tri-Level Complex Wave* is seen as an integrated whole, and analogous to the I-Ching hexagram that functions as a holistic entity, but contains the individual expression of hexagram, trigram, and line (yin or yang). In order to establish this tri-level expression mathematically, we combine the complex waves of the linear, trigrammatic, and hexagrammatic levels of expression. The general equation expressing the summation of the three wave levels is written as follows:

$$y_T(x) = \text{lin}(x) + \text{tri}(x) + \text{hex}(x) \quad [74]$$

Substitutions in [74] for  $\text{lin}(x)$ ,  $\text{tri}(x)$ , and  $\text{hex}(x)$  from equation [43], [60], and [72] give us:

$$y_T(x) = y_{C1}(x) + y_{C3}(x) + y_{C6}(x) \quad [75]$$

and further substitutions from [43], [60], and [72] give us the defining expression for the *Tri-Level Complex Wave*:

$$\begin{aligned} y_T(x) = & \left\{ - \left[ \frac{\Delta y_{r(i)} + \Delta y_{f(i)}}{\Delta x_{f(i)}} \right] * [x] + \left[ \frac{\Delta y_{r(i)} x_{(i+1)} + \Delta y_{f(i)} x_i}{\Delta x_{f(i)}} \right] + (y_{r(i+1)} - y_{f(i)}) \right\} + \dots \\ & + 3 \left\{ - \left[ \frac{\Delta y_{r(j)} + \Delta y_{f(j)}}{\Delta x_{f(j)}} \right] * \left[ \frac{x+2}{3} \right] + \left[ \frac{\Delta y_{r(j)} x_{(j+1)} + \Delta y_{f(j)} x_j}{\Delta x_{f(j)}} \right] + (y_{r(j+1)} - y_{f(j)}) \right\} + \dots \\ & + 6 \left\{ - \left[ \frac{\Delta y_{r(k)} + \Delta y_{f(k)}}{\Delta x_{f(k)}} \right] * \left[ \frac{x+5}{6} \right] + \left[ \frac{\Delta y_{r(k)} x_{(k+1)} + \Delta y_{f(k)} x_k}{\Delta x_{f(k)}} \right] + (y_{r(k+1)} - y_{f(k)}) \right\} \quad [76] \end{aligned}$$

Equation [76] is the defining equation for the *Tri-Level Complex Wave*. This expression takes one from the individual elements of the *linear complex wave*, up to the *trigramatic* and *hexagramatic complex waves*, and finally to the *tri-level complex wave*. Notice that the subscripts  $j$  for the trigramatic section, and  $k$  for the hexagramatic section of equation [76] have replaced the subscript  $i$  in equations [60] and [72], as they have been defined in equations [61] and [73]. We now have a complete and well-defined function for our *Tri-Level Complex Wave*, or *data set*.

Equation [76] produces a tri-level wave number set that contains some negative values. The 384 number *data set*, on the other hand, is the set of positive real numbers in the domain  $0 \leq x \leq 384$ . This means that part of the “raw” data set produced by equation [76] lies outside the  $y$ -value domain that is thought to be the proper expression of this waveform. One procedure that is widely used for converting negative values of some arbitrary waveform, into positive values, is the use of the absolute value operator. If one views this *tri-level complex wave* as some kind of information carrying signal, like an amplitude modulated radio wave, for example, then a valid procedure for processing such a signal is the application of the absolute value operator. In the rf signal processing case, the received modulated-carrier waveform is passed through absolute value circuitry (rectifier) so that the negative values of the wave are converted to positive values. This actually improves the signal to noise ratio of the carrier envelope, which is the information carrying modulation signal. This “rectified” signal is then processed by a detector circuit that extracts the information carrying modulation wave from the carrier wave. Although the tri-level wave and the radio wave are not strictly analogous, they appear similar enough to make a plausible argument for the application of the absolute value operator here. This operation is expressed as:

$$y_{DW} = \text{ABS}[y_T] \quad [77]$$

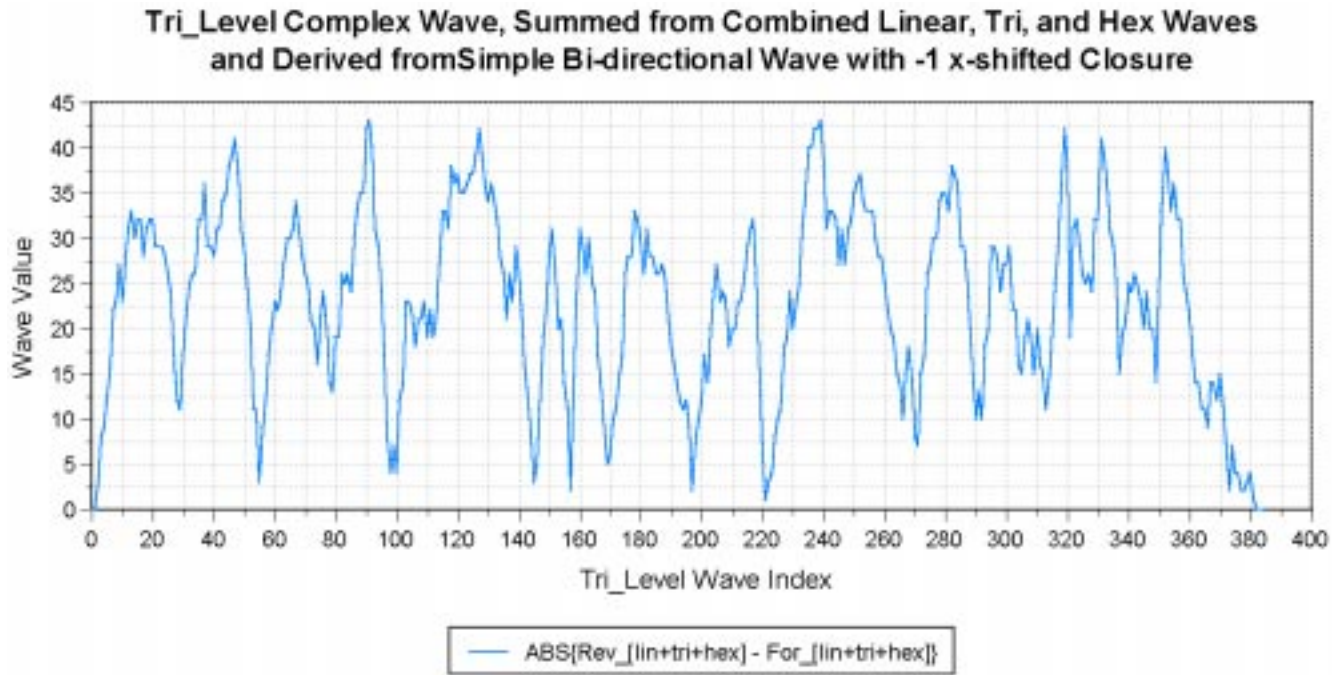
Where:  $y_{DW}$  is the *Data Wave* that is graphed in Fig. 11, and defined as the absolute value of the *Tri-Level Complex Wave* as expressed in equation [73]. This number set is used as input data for the *TimeWave Zero* software, which performs an infinite series expansion that Meyer calls a *fractal transform*<sup>11</sup>, to generate the *TimeWave* viewed on the computer screen.

## Standard and Revised Data Set Comparisons

With equation [73] and [74], and the graph in Fig. 11, we have completed this formalized development of the *TWZ data set*. We are now in a position to compare these results with those of the standard development reported by McKenna and Meyer in *the Invisible Landscape* and the *TimeExplorer* manual, as well as address the issues raised by the *Watkins Objection*.

Fig. 12 is a graph of both the *standard* and *revised data sets*, and it shows some remarkable similarities as well as significant differences. One interesting feature of this graph, is the nature of each wave at its respective endpoints. Recall that the value of the

wave at  $x = 0$  will be discarded because it is a duplicate or “wrap” of the value at  $x = 384$ . This will not effect the relative values of the two waves at  $x = 384$ , because they are both zero-valued at this endpoint. However, the value of each wave at  $x = 1$  is not the same, with the *standard wave* having a value of 10 while the *revised wave* value is zero.

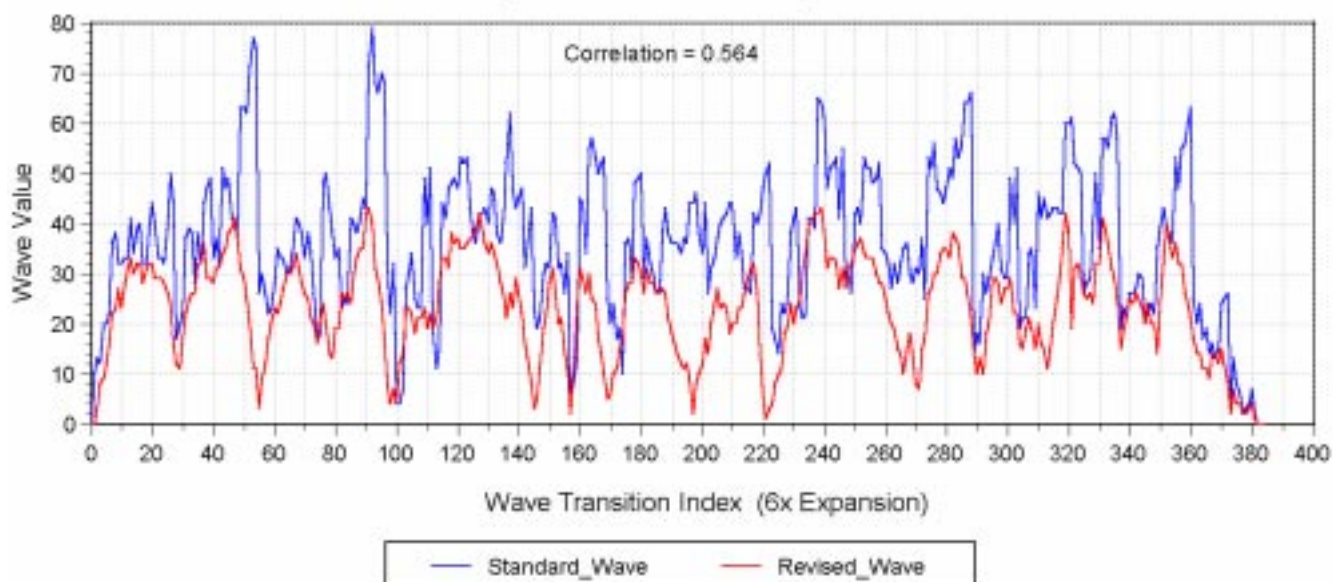


**Figure 11**

Why does this matter, you may ask, since there are many obvious differences between the two waves – what is the significance of this difference? For the *standard wave*, it has been argued that the zero value at the end of the waveform implies some kind of singularity at the end of the process – or at the end of time. This *revised wave* is implying, however, that there may be singularities at *both* ends of the continuum. This is Also an argument for a *closed* system that may be undergoing some kind of cyclic renewal process – perhaps each cycle expressing ever higher ordered states of complex form, or *Novelty*.

There are concepts emerging from the field of quantum cosmology that may describe an analogous cyclic process. This is theory in which universes are treated like quantum particles that inhabit a larger, or higher dimensional domain called a *multiverse*. Michio Kaku<sup>12</sup>, a theoretical physicist and co-founder of string field theory, has described a process where universes emerge from the zero-point, or vacuum field, go through an evolutionary process, then perhaps return to the zero-point field at the end of the cycle. This cycle may then repeat itself, possibly with increased complexity and *Novelty*. So could this be similar to the process that the *TimeWave* and *Novelty Theory* attempt to reveal? Perhaps further investigation into the nature of the TimeWave will shed some light on these questions.

### Comparison of Standard and Revised Tri-Level Complex Waves Showing Common and Divergent Features



**Figure 12**

Another significant feature of Fig. 12 is the apparent agreement of the two waves in the lower frequency domain. Frequency content of any waveform expresses itself as variations in the rate of change of its value as the wave propagates in some realm, that could be either a space or time domain, or both. So the slope of a waveform at any given point, or its general shape, can reveal frequency content (the magnitude and rate of specific underlying processes). Examination of the wave pair in Fig. 12 shows that there is a common lower frequency process occurring for each waveform. The higher frequency processes appear as relatively shorter duration peaks riding upon the slower process. The lowest frequency process occurring in these waveforms can be seen by drawing an imaginary line between the highest of all the peaks as one moves over the domain of the waveforms. Slightly higher frequency components can be seen by drawing that imaginary line over the peaks and valleys upon which the sharpest and shortest duration peaks ride. The graphs do differ in the higher frequency domain as can be seen by the steeper slopes of the largest *standard wave* transitions. This could very well be due to high frequency noise present in the *standard* data set because of the imbedded mathematical errors.

The low frequency, or long duration processes, are those that may occur on the scale of millennia or even billions of years, whereas the higher frequency processes may occur on the scale of a human lifetime. Could it be that the lowest frequency process is the signature of some creative principle at work, be it strange attractor, zero-point field, or *eschaton*. Could this creative energy, be perturbing the fabric of space-time in such a way as to trigger the creation and conservation of higher ordered states – something like the gravitational energy of a passing nearby star triggering the formation of a comets from the Ort cloud? Is this lowest frequency process then a kind of ground state, upon which all higher frequency processes express themselves? Perhaps in time these questions will be answerable, although certainly not today.

An obvious feature of Fig. 12 that clearly shows in this graph, is the difference in the average wave value between standard and revised waves. The average wave value for the standard wave is somewhat greater than the average value of the revised wave. This difference in average wave value appears to be the result of differences in the higher frequency components of the wave pair, perhaps due to noise in the standard wave that is produced by the mathematical errors that are present. These high frequency components of the standard wave show up as the steep peaks that rise well above the peaks in the revised wave. In the Fourier analysis that follows, these large peaks appear as high frequency noise that adds randomness to the wave. The impact of this difference on the final TimeWave, is to shift the average level of novelty upward (lower values) from that expressed by the standard wave. In other words, the revised wave expresses a process with somewhat higher levels of novelty, than does the standard wave. Since *Novelty* isn't a calibrated process, it's not possible to determine what the more "reasonable" level of *Novelty* would be. All that can be expressed then, is relative Novelty.

One final feature of Fig. 12 that requires some discussion, is the correlation number at the top of the graph. In order to determine and quantify the degree of interdependence, or inter-relatedness of the standard and revised waveforms, a mathematical operation called *correlation* was performed with these two number sets. The number at the top of the graph is the result of that analysis – a value of 0.564. A correlation of 1.0 would mean that the waveforms are identical, whereas a correlation of zero would indicate no functional relationship between the two. Additionally, a correlation of  $-1$  would indicate that the waveforms were mirror images of one another – a peak reflected by a trough etc. In this case a correlation of 0.564 indicates that these two waveforms show a significant level of interdependence, although far from identical. This level of correlation could be considered likely for two number sets that share a common origin, as well as sharing many of the same developmental procedures.

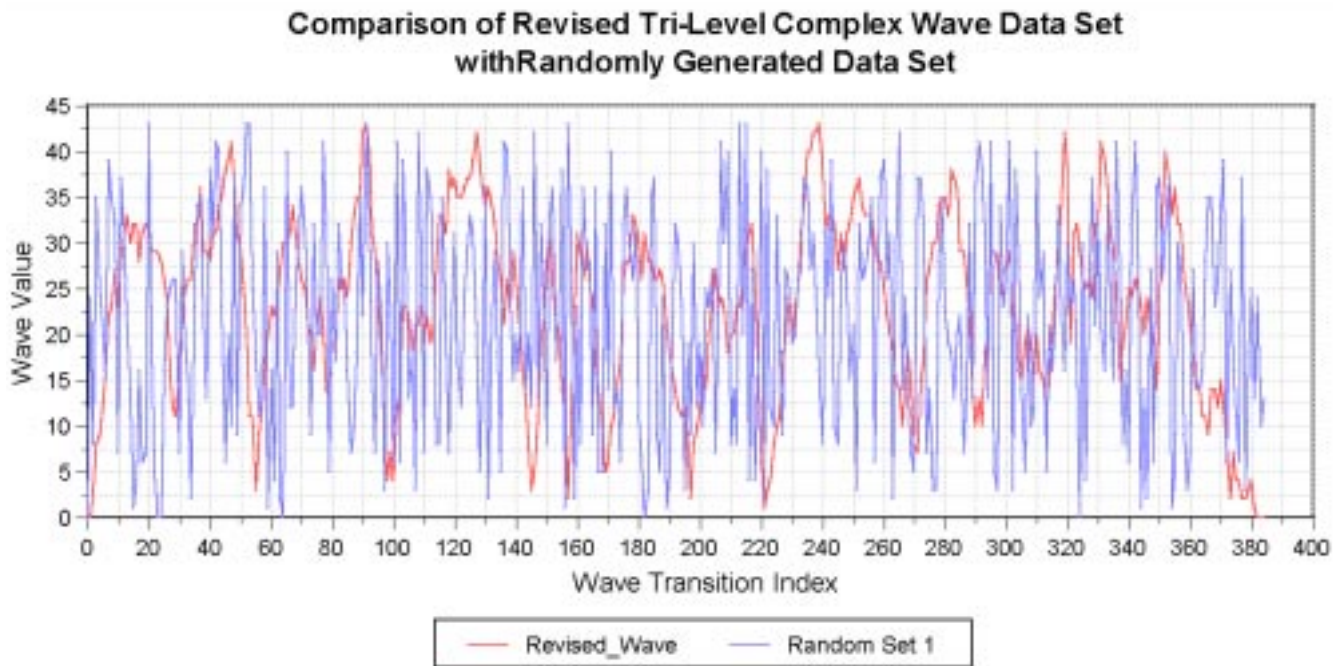
## Data Wave and Random Number Set Comparisons

One method for assessing the information carrying potential of the *Data Wave*, and convincing oneself that it is not a random process, is to compare it with a data set that has been randomly generated. Several such *random wave* sets were consequently produced to be compared with the revised and standard *Data Wave* number sets directly, and to also use as input to the TWZ software to generate random seeded TimeWaves. Fig. 13 is a graph of the revised *Data Wave* with a random wave set overlay, and it clearly shows that these number sets bear little resemblance to one another. Correlation analysis of the two sets shows a correlation of 0.03, or essentially un-correlated as one would expect for any random number set. Fig. 13 also appears to show that the revised *Data Wave* is a very different type of number set from the random wave set, and it appears to showing some kind of information carrying process. Is this in fact the case, or does it just appear that way?

Examination of the *power spectra* for the *data* and *random waves* shown in Figs. 12 and 13 can reveal something about the nature of these three waveforms and their



relationship. The conversion of time, or space domain waveforms into frequency domain waveforms (frequency spectrum or power spectrum) is performed using a mathematical operation called a Fourier transform. With this method, a frequency spectrum can be produced, which can tell us how much power is contained in each of the frequency components (harmonics) of a given waveform, and thereby providing the frequency distribution of the wave power. This distribution would typically be different for information carrying waveforms than for random, or noise signals. The random, or noise signal spectrum is typically flat over the signal bandwidth, and often distinguishable from an information carrying signal spectrum that exhibits  $1/f$  ( $f$  = frequency) behavior.

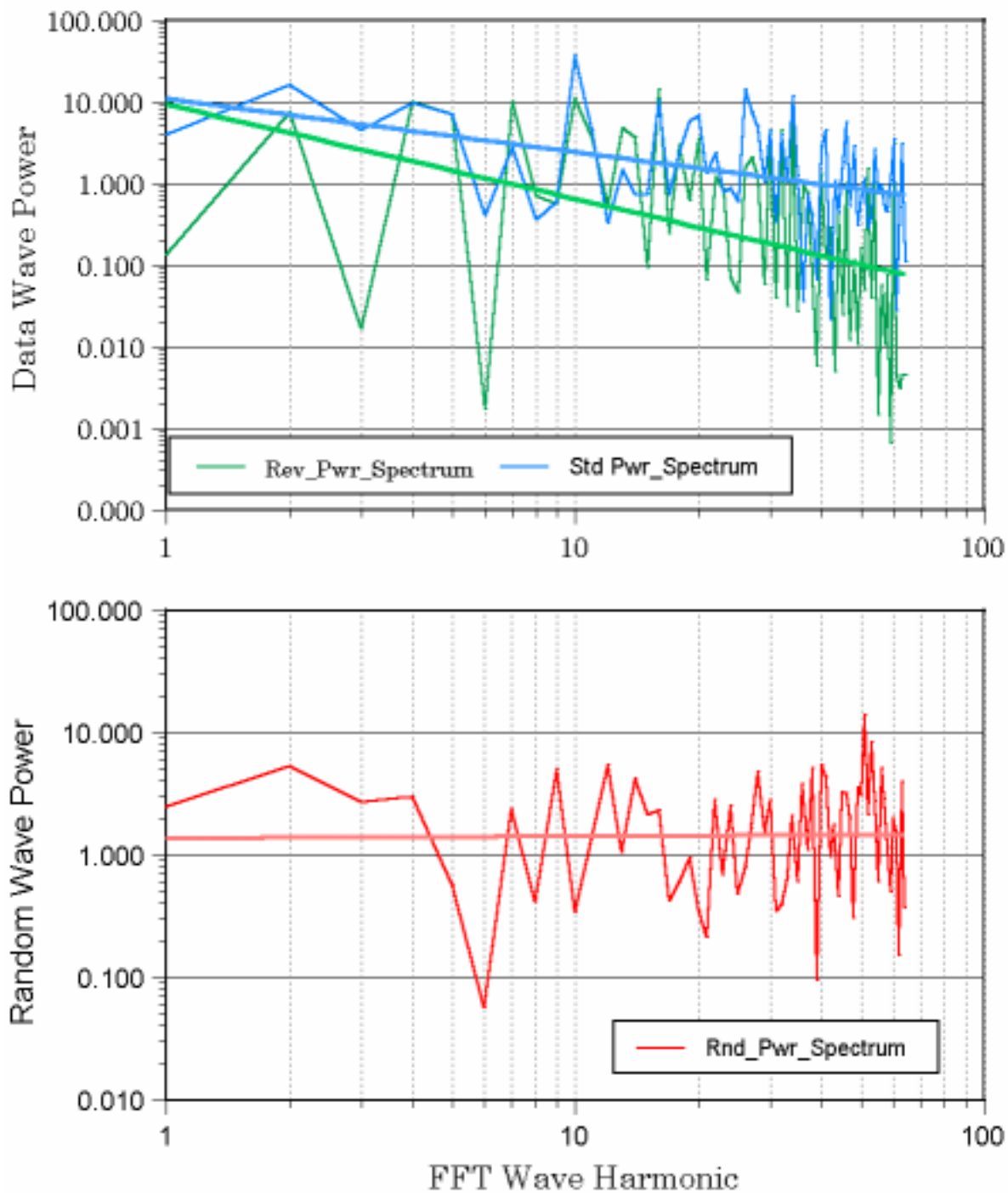


**Figure 13**

Fourier transform operations were performed on the data sets shown in Figs. 12 and 13, with the results shown in Fig. 14. The top graph of Fig. 14 includes plots for the *standard* and *revised Data Wave* power spectra, while the bottom graph displays the *Random Wave* power spectrum. The colored lines drawn through each of the spectra are *power function* curve-fits, that show the frequency roll-off characteristics of each wave. Notice that the two power spectra in the top graph exhibit frequency roll-off (power level decreases with increasing frequency), whereas the lower graph power spectrum exhibits a flat frequency response (power level is frequency independent). This frequency roll-off is characteristic of information carrying signals, whereas the flat response is characteristic of noise or random signals.

The *revised data wave* spectrum, shown in the top graph in green, is exhibiting the nearly perfect  $1/f$  frequency response that is typical for an information carrying waveform. On the other hand, the *standard data wave* power spectrum shown in blue, exhibits frequency roll-off, but with a flatter response that is not  $1/f$ . In fact, the flatter

## FFT Power Spectrum Comparison for Data Wave and Random Data Sets



**Figure 14**

frequency response of the *standard data wave* is the likely result of high frequency noise that increases the power at the tail end of the spectrum and prevents a steeper roll-off. This is something that should be expected from the distorted *standard data wave* with imbedded mathematical errors, which would tend to add randomness to the wave. The signature of such randomness can be seen in the *Random Wave* power spectrum, shown in the lower graph in red. This plot shows the typically flat frequency response of a

random, or noise signal with no information content. Apparently, the graphs in Fig. 14 are showing that the standard and revised data *waves* are definite information carrying waveforms, but that the distorted *standard data wave* has imbedded high frequency noise that flattens its response. This is essentially what Figs. 12 and 13 are showing as well.

## Standard, Revised, and Random Generated TimeWave Results

### (1) The TimeWave Zero Screen Set Comparisons

Once the *Data Wave*, or 384 number data set has been generated, it becomes the input data for the *TimeWave Zero* software package. As mentioned previously, the software performs what has been called a *fractal transform*, or expansion of the 384 data number set to produce the *TimeWave* viewed on the computer screen as a graph of *Novelty*. In order for this fractal expansion to be performed properly, the software requires that the 384 number data set shown in Fig. 10 be reversed, such that data point 384 becomes data point 1 and data point 0 is discarded (since it's a duplicate or wrap of data point 384).

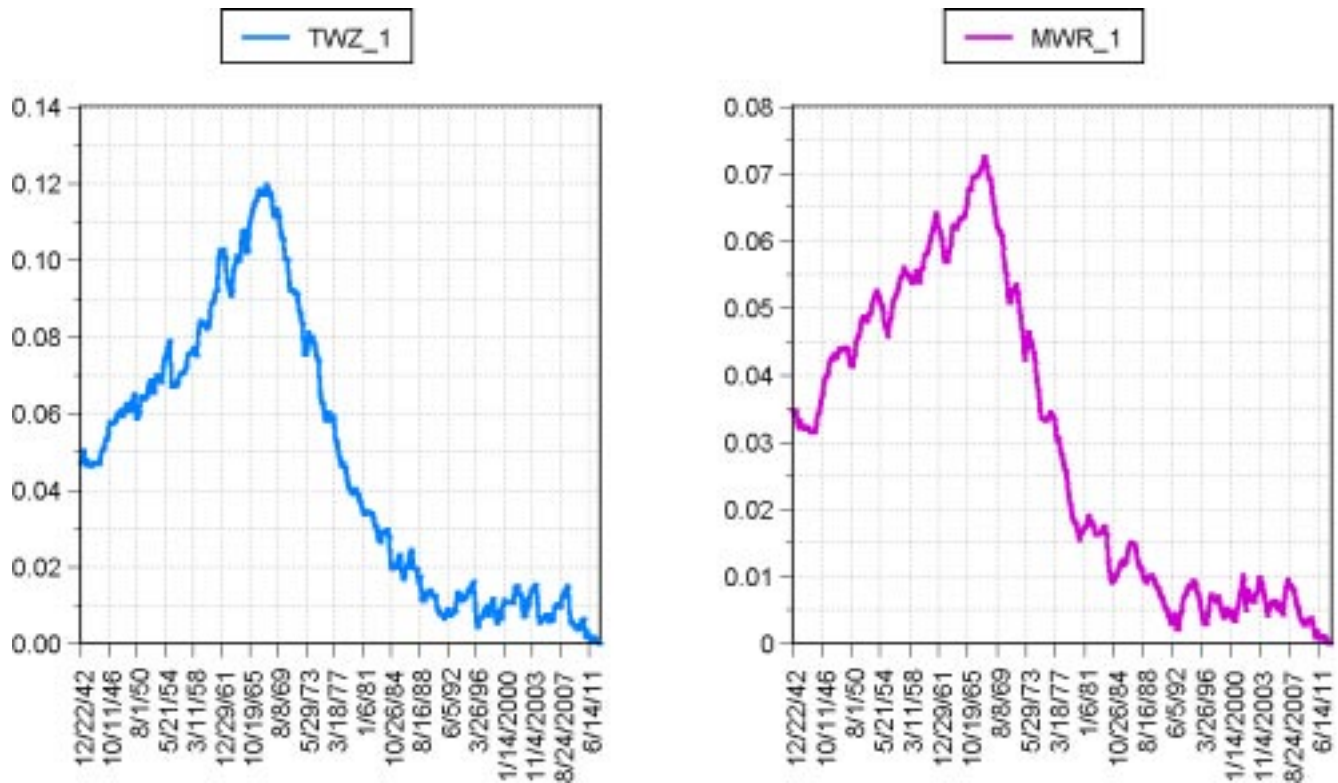
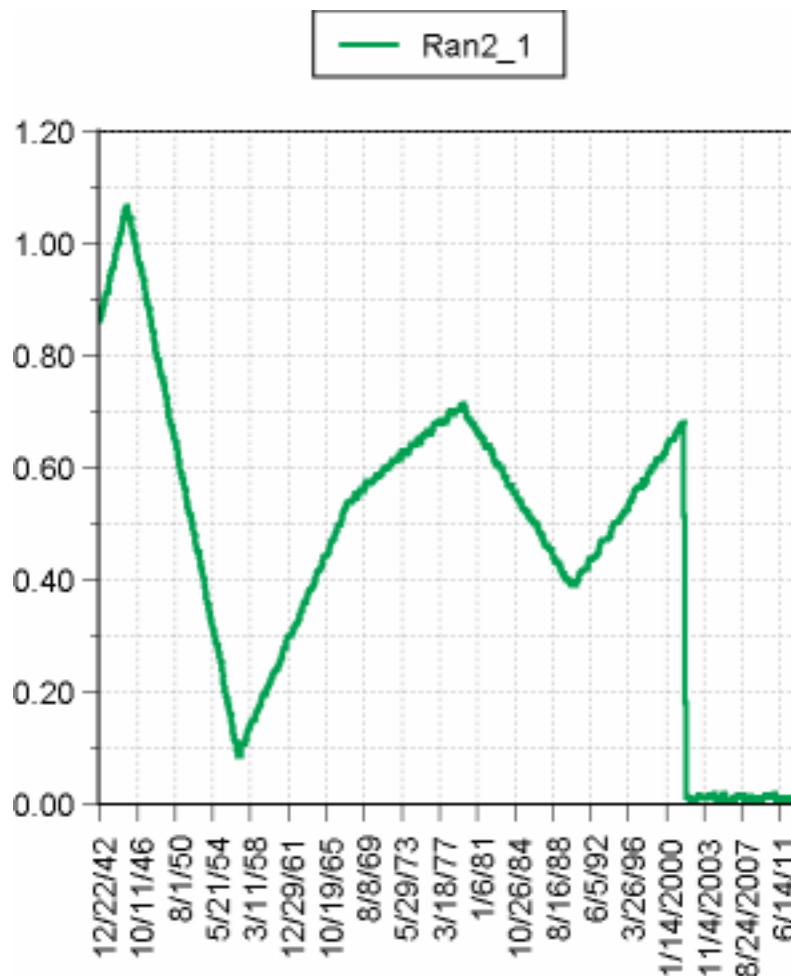


Figure 15a

Three separate data sets were used in order to generate the *TimeWaves* needed for comparison – the *standard* data set, the *revised* data set, and a *random* data set. The results of some of these *TimeWave* comparisons will be shown in the graphs that follow, beginning with the default *TimeWave* graphs that are included with the *TimeExplorer* software as pre-computed waveforms.

Figs. 15a and 15b show the *TimeWave* that is stored by the software as Screen 1, and it covers the period between 1942 and 2012. Fig. 15a shows both the *TimeWave* resulting from the *standard* data set on the left, and that for the *revised* data set on the right. On the other hand, Fig. 15b is the *TimeWave* generated by the *random* data set, and it clearly bears little resemblance to the graphs of Fig. 15a.

This is the *TimeWave* graph that McKenna has called “history’s fractal mountain”, because of its mountain-like shape. There are several features to notice here, with the first being that these two plots have remarkably similar shapes – obviously not identical, but there is clearly a common dominant process at work. Another common feature of significance shown in these two graphs, is that the major decent into *Novelty* (peak of the mountain) begins sometime in 1967. Finally, as mentioned earlier, the *TimeWave* produced by the *revised* Data Wave number set, shows a higher average level of *Novelty* for this time period (lower values), than does the *TimeWave* produced by the *standard*

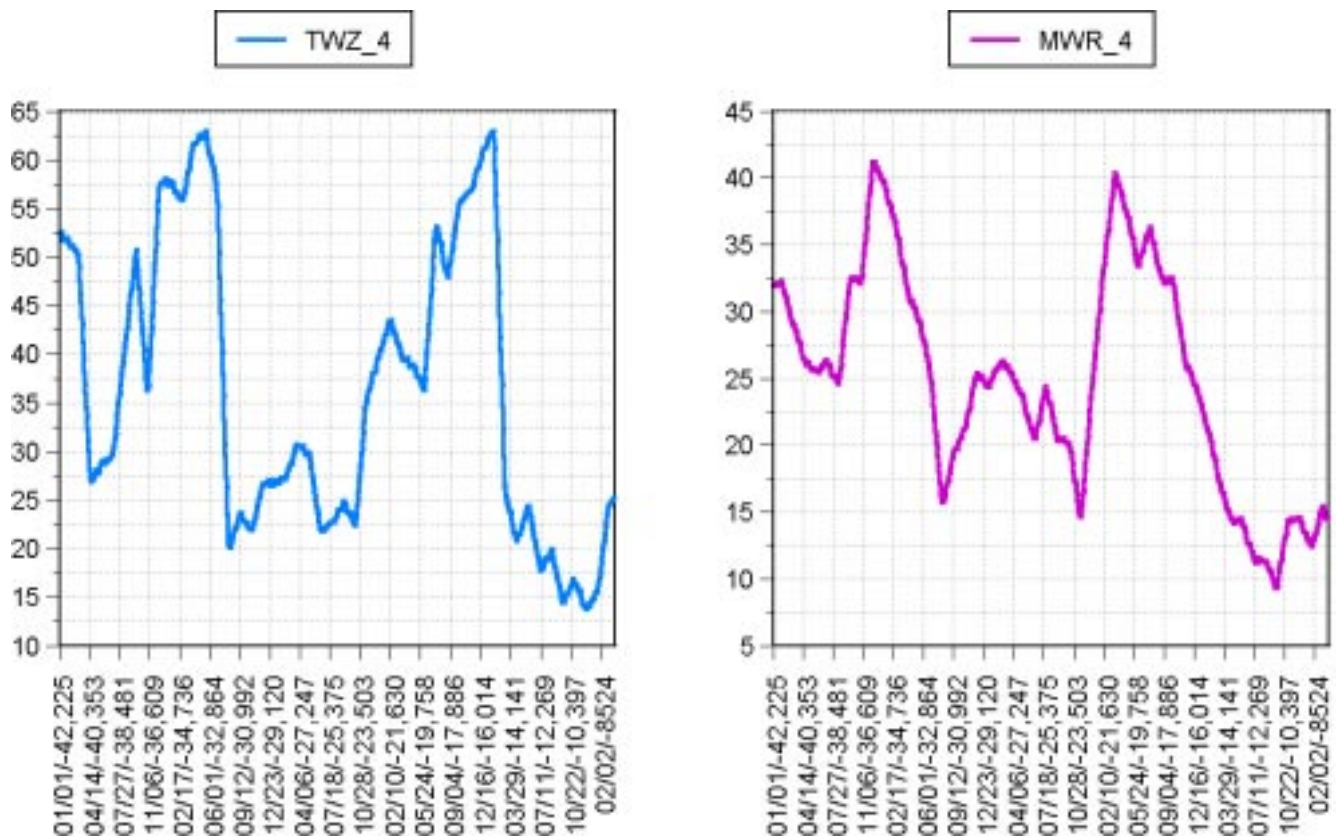




**Figure 15b**

*data* set. This *Novelty* difference is the likely result of the *standard wave* distortion, caused by the imbedded mathematical errors that produce significant high frequency noise in the wave. As shown in Fig. 14, the high frequency components of the revised data wave are lower than the standard wave by an order of magnitude.

Fig. 16a shows the standard and revised TimeWave graphs for Screen 4 of the TWZ display. Again, these two plots are quite similar in terms of their appearance, and seem to be showing evidence of some common underlying process. The differences may be due to the fact that the standard number set produces more high frequency noise because of the imbedded errors in the number set. The correlation between these two graphs was



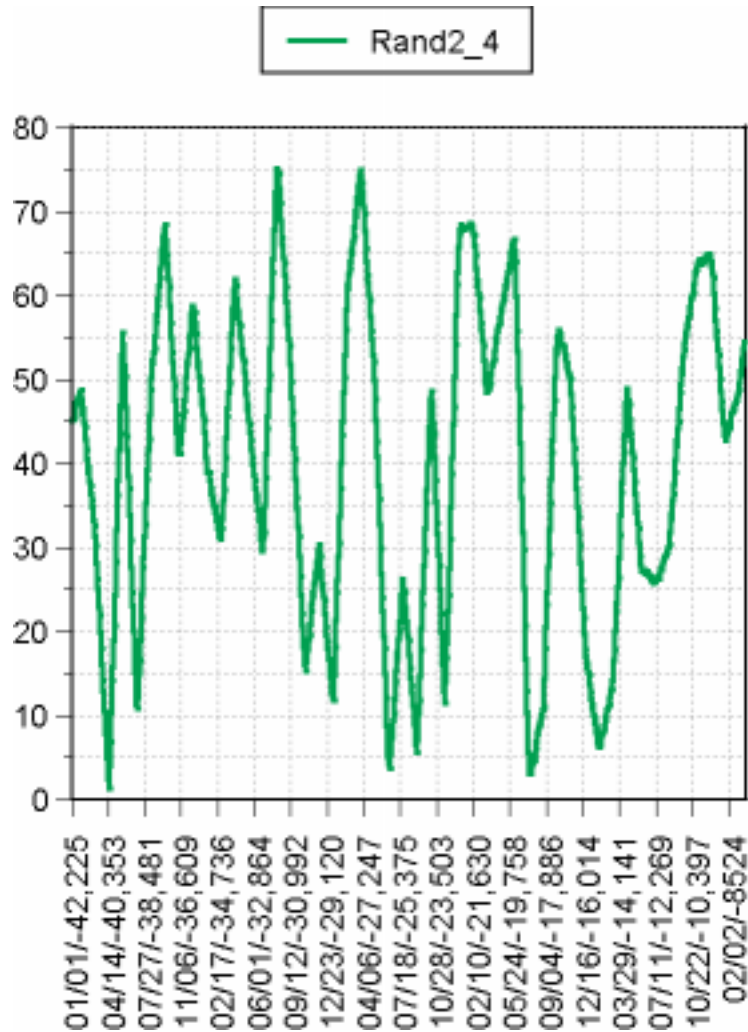
**Figure 16a**

found to be 0.731, not as high as Screen 1, but still a significant correlation nonetheless. On the other hand, the random data set TimeWave shown in Fig. 16b, shows very little correlation with either of the graphs in Fig. 16a. This is expected, since random number sets are by definition, un-correlated with any other number set.

A complete set of comparisons like those shown in Figs. 15 and 16 were performed on all the TimeWave Zero screen sets (Screens 1-10) with very similar results. The correlation results for the TWZ Screen set comparisons ranged from a low of 0.73 to a high of 0.98



with an average correlation of 0.86, showing that the standard and revised TimeWaves in this screen set were remarkably similar. This was not the case for other TimeWaves that were examined, which will be shown later. In other cases of *TimeWave* comparison, the differences between the standard and revised waves, appears to show that the *revised TimeWave* expresses a *Novelty* process having better alignment with known historical process – something one would expect from a more precise formalization process. More analysis is certainly in order, but the data thus far seems to make that case.

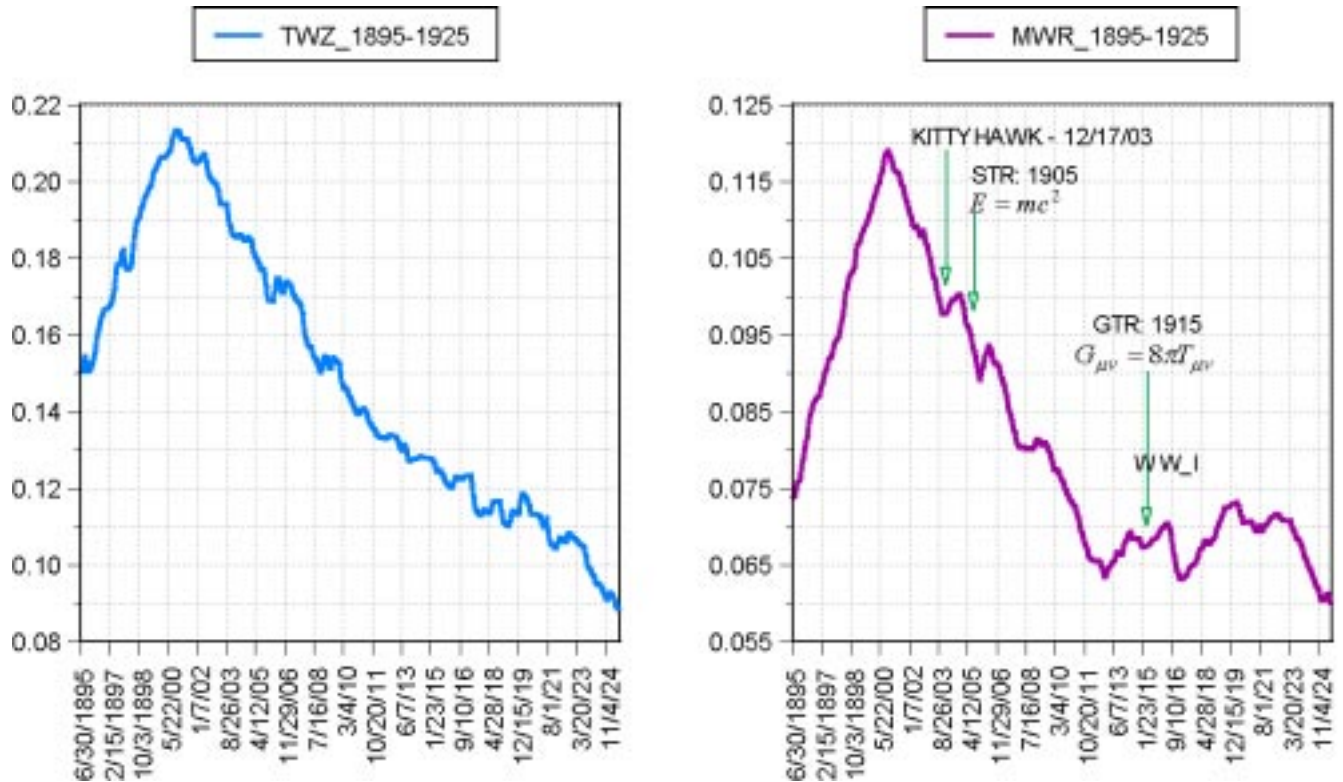


**Figure 16b**

## [\(2\) Comparisons for Other Significant Historical Periods](#)

Several other TimeWave periods having historical significance were examined for comparison, but the two reported here are the periods from 1895-1925, and from 1935-1955. The first period includes major advances in physics and technology, as well as a world war; and the second period includes the development and use of nuclear weapons, as well as two major wars. Fig. 17 is a graph of the TimeWave comparison for the 1895-

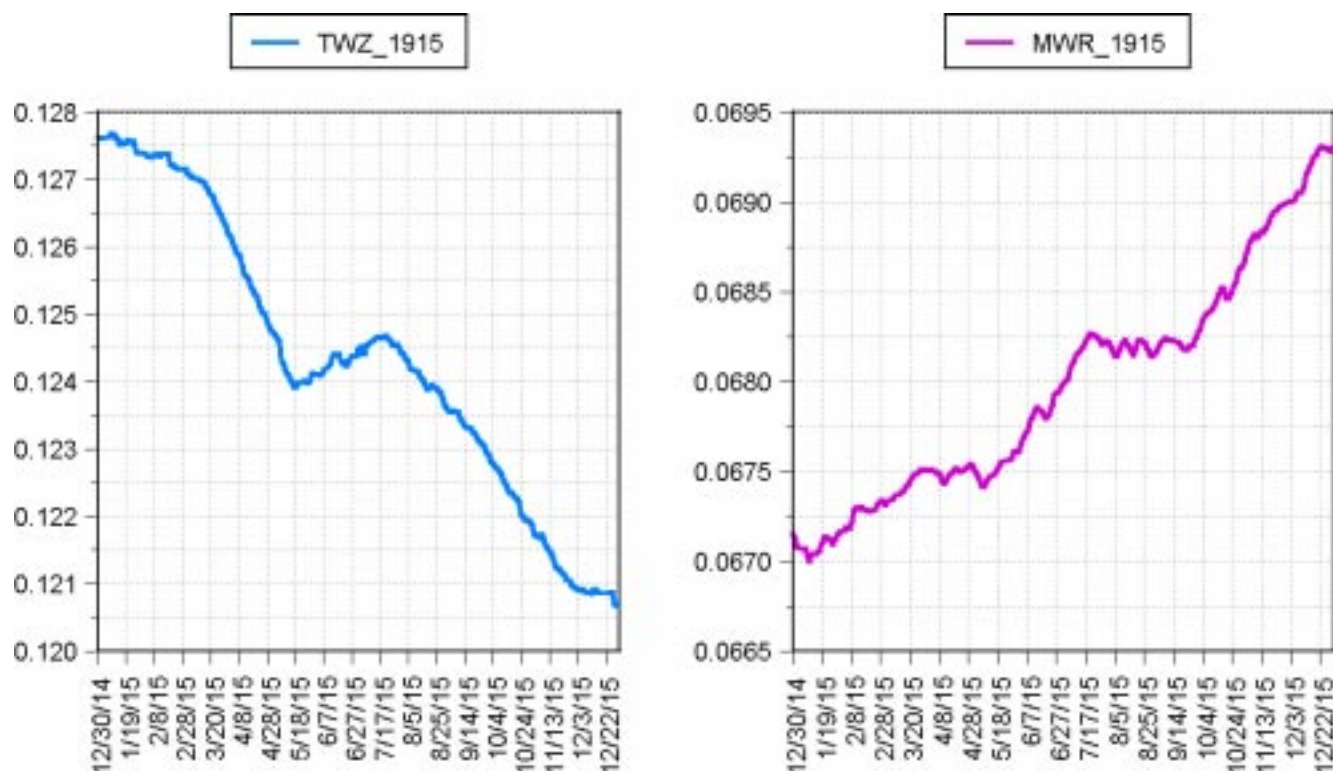
1925 period, and again these plots are remarkably similar in form. Several significant dates are marked with green and red arrows to signify *Novel* and *Habitual* phenomena. The first powered flight happens at Kittyhawk on December 17, 1903; followed by Einstein's Special Theory of Relativity (STR) on June 30, 1905; General Relativity in 1915, and the World War I period of 1914-1918. The events that would be considered novel (manned flight and breakthroughs in physics) all occur at Novelty troughs or Novelty descents. The Habitual phenomenon (war), on the other hand, appears to drive what seems to be a very novel period, back into habit. When both novel and habitual phenomenon are occurring simultaneously, they both influence the shape of the TimeWave. WWI may have driven the wave further into habit than it did, if it weren't for the simultaneous occurrence of very novel phenomena. For example, the work on the General Theory of Relativity occurs in the midst of World War I with its "same 'OLE'" habitual nature. The more novel process of a significant advancement in scientific knowledge, actually appears to suppress what would be a major ascent into habit, and actually driving the wave into novelty troughs.



**Figure 17**

Notice that the standard TimeWave on the left doesn't show the regression into habit during the First World War – the revised TimeWave clearly does. This is one case in which the revised TimeWave appears to provide a better description of the Novelty process than does the standard TimeWave. However, this is something that should be expected for a process with a more precise and consistent mathematical model.

Fig. 18 shows the 1915 time period, for which the two waves exhibit a substantial disagreement. With the exception of a brief two-month period, the standard TimeWave shows a steady descent into Novelty. The revised TimeWave, however, shows more of what one might expect for a planet embroiled in global conflict. Additionally, the revised TimeWave shows several instances where the determined march into habit is either slowed or temporarily reversed; and with the publication of the general theory in early 1916, the level of Novelty becomes too great for the forces of habit, and the wave plunges. This figure provides a good example of how the standard and revised TimeWaves can exhibit behavioral divergence, and how this divergence tends to affirm the improved accuracy of the revised waveform. Let us now take a look at another period that most of us are familiar with – the period that includes World War II, nuclear energy development, and the Korean War.



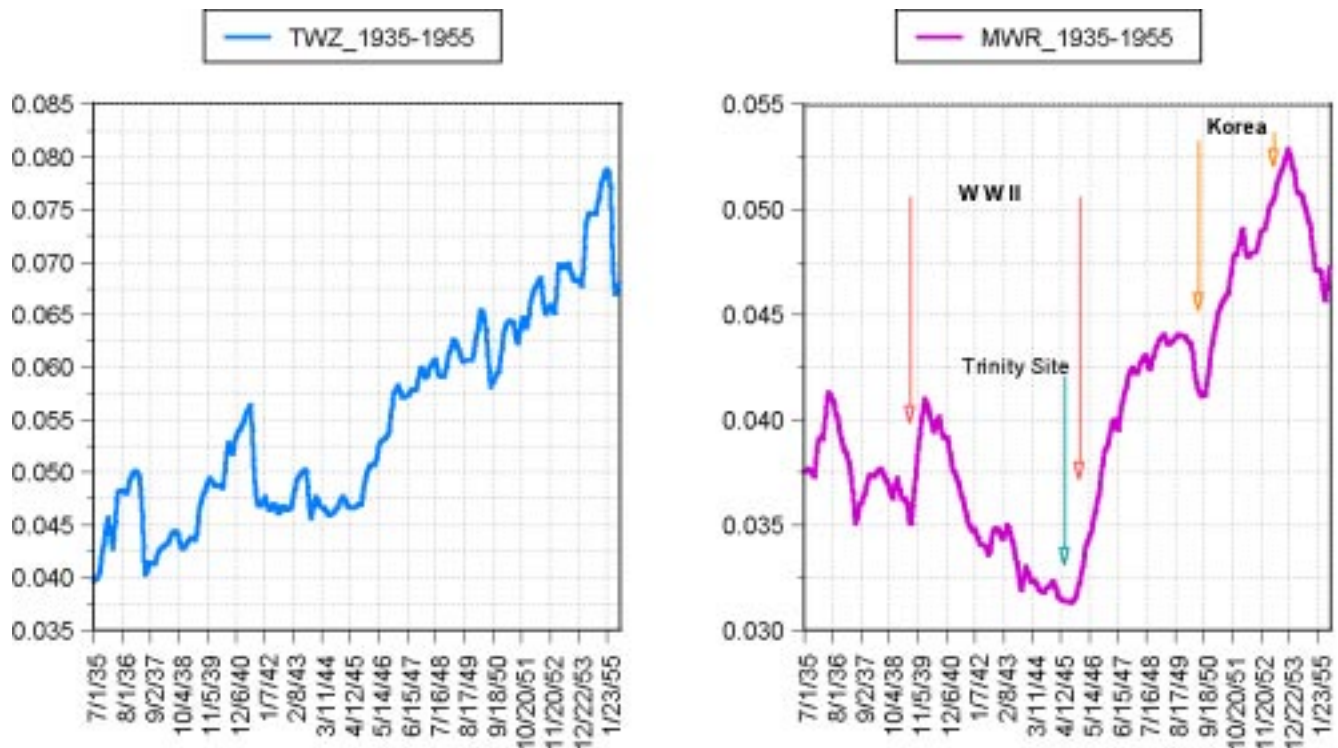
**Figure 18**

Figure 19 shows the standard and revised TimeWave comparison graphs for the period 1935-1955, and there are obvious similarities and clear differences between the two waves. Both graphs show that WWII begins and ends during steep ascents into habit, but they describe somewhat diverging processes, for much of the middle period of the war. The revised TimeWave shows that a very novel process is apparently at work for much of the period of the war. The standard TimeWave does show novel influences, but it is neither as consistent nor dramatic as for the revised TimeWave. Some very potent novel process seems to be occurring during much of the war period, and that process may be suppressing a major ascent into habit that might otherwise be happening. Could this novel process be the development of nuclear science and technology, eventually leading

to the production and use of nuclear weapons? That may be an offensive notion, but let's take a closer look at it.

The development of nuclear science is really about becoming more aware and knowledgeable of a process that powers the sun and the stars – more aware of just how a very powerful aspect of nature works. What one then does with such knowledge is a different process entirely – and largely a matter of consciousness and maturity. As we can see from the revised TimeWave graph, the moment that this knowledge is converted to weapons technology – the nuclear explosion at Trinity Site in New Mexico – the wave begins a steep ascent into habit.

The use of this awesome power against other human beings in Hiroshima and Nagasaki occurs shortly after the test at Trinity Site, and occurs on a very steep ascending slope of habit. Perhaps the process of becoming more aware of nature, and ourselves – is very novel indeed. It is the sacred knowledge of the shaman, who returns from an immersion into an aspect of nature, with guidance or healing for her or his people. We seem to have lost the sense of sacred knowledge with its accompanying responsibility, somewhere along the way. Perhaps it is time to regain that sense, and reclaim responsibility for our knowing.



**Figure 19**

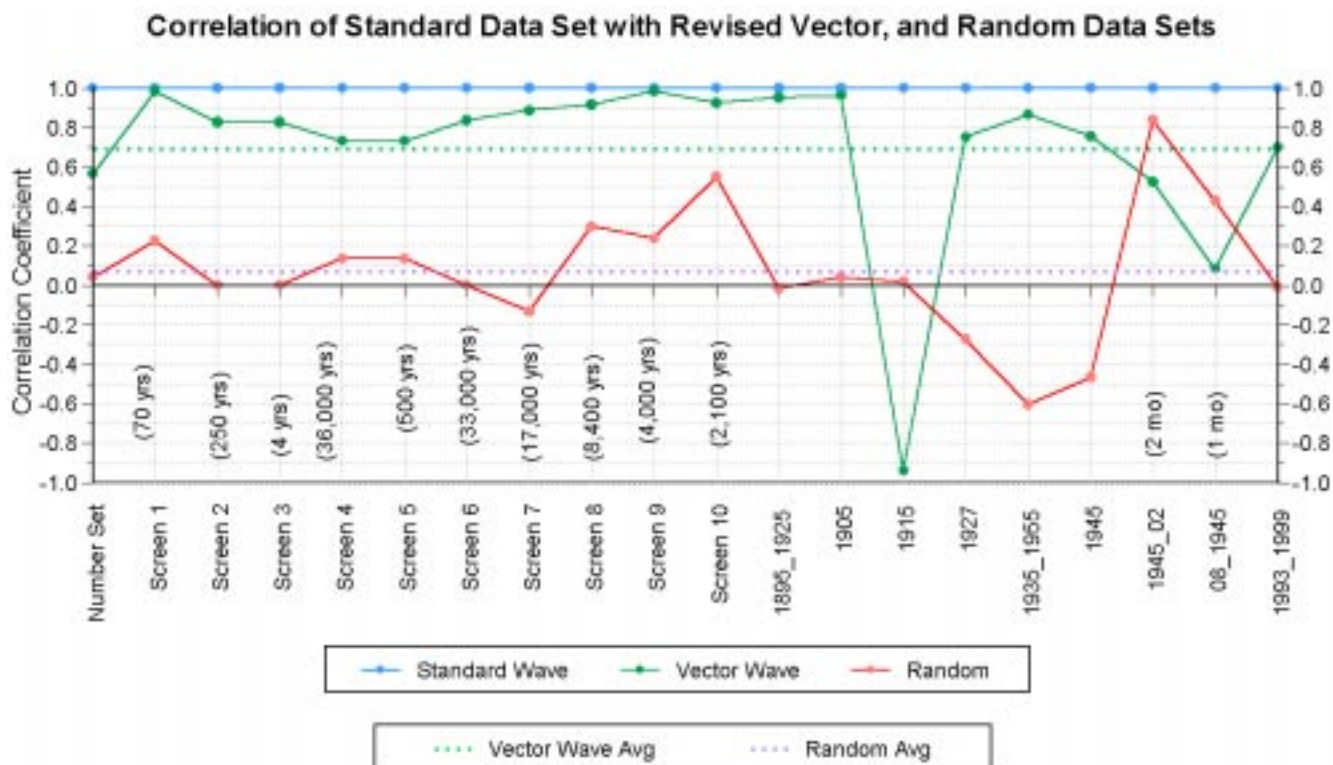
The revised TimeWave of Fig. 19 also shows the period of the Korean war as a very steep ascent into habit, although something occurring early in 1952 did momentarily reverse the habitual trend.



## Correlation Data and TimeWave Comparisons

Correlation analysis was performed for all the data sets compared in this report, as well as the remaining eight TWZ screen sets not shown here, and selected time periods. This type of analysis allows us to examine the relationship between data sets, and estimate their degree of interdependence – i.e. how similar their information content is. The results of these analyses are shown graphically in Fig. 20, and they include the ten *TimeWave* screens included with the TWZ software, nine selected historical windows, and the 384 number data sets. In all cases shown, the revised and random data sets are being correlated (compared) with the standard data set. Since any number set correlated with itself, has a correlation coefficient of one, the blue line at the top of the graph represents the standard data self-correlation.

Recall that a correlation of 1 signifies number sets that have identical information content, a correlation of zero signifies no common information content, and a correlation of  $-1$  means that the number sets information content exhibit “mirror image” behavior – wave peaks to wave valleys etc. The green line in the graph shows the degree of correlation between the revised waveform and the standard waveform, for each of the separate TimeWaves that were examined. The red line shows the correlation level between waves generated by the random seeded data sets, and those generated by the standard data set. The first point of each line, is the correlation coefficient for each of the 384 number data sets examined – *random*, *revised*, and *standard* data sets.



**Figure 20**



The first feature to notice about the *revised* and *standard* data set correlations shown in Fig. 20, is the fact that the revised 384 number data set shows a correlation with the standard number set of about 60% - a comparison that is shown in Fig. 12. This is a significant cross-linking of information content, but something that one might expect for number sets with a common base and very similar developmental procedures. The next feature of significance is the fact that the correlation between the *revised* and *standard TimeWaves*, for all ten TWZ screen sets, is better than 70% and as high as 98%, showing a very high level of interdependence. The time periods represented by these ten TimeWave screens, ranges from 4 years to 36,000 years, which is labeled on the graph. The duration of these TimeWave periods may have a bearing on the level of correlation, as we shall see in a moment.

Beginning with the period 1895-1925, the graph shows more scatter in the correlation between standard and revised data sets, which ranges from about 98% down to 8%, with one anti-correlation of -95%. Notice that the correlation appears worse for very short time periods, one to two months or so. One possible explanation is that the very short time period TimeWaves are generated by a very few data points – in other words a low wave sampling frequency or rate. A small, and under-sampled input data set would add a higher level of noise to the wave signal, and consequently produce the higher data scatter observed. The sampling theorem, from information theory, states that aliasing (noise generation) begins to occur when the signal sampling rate becomes less than twice the highest frequency component of the sampled signal. This is certainly something that may be occurring in the mathematics of TimeWave generation.

Additionally, as mentioned previously, this difference could be the consequence of having an improved model of the process. It is important to remember through all of this comparison analysis, that the standard data set is generated by a process with imbedded flaws - not enough to destroy the information content of the wave signals, but enough to cause some distortion of that information content. This correlation analysis is interesting, primarily because it leaves the standard *TimeWave* intact, more or less – but the important point to remember is that even with low correlation the *revised data set* appears to produce a better *TimeWave*.

It is probable that the variations we observe in Fig. 20 are the result of both the distortion of the information content of the 384 number *data set*, as a result of mathematical errors, and the low data wave sampling rate that occurs for short duration *TimeWaves* (an unexamined but plausible thesis). It is also important to point out here, that when we do see significant differences in the TimeWaves generated by the *standard* and *revised* data sets, those differences have revealed a *revised* TimeWave of greater accuracy. However, it is important that we examine a significant variety of additional TimeWave periods, to gather more statistics on the functioning of the revised wave; but the data in hand so far, seem to be suggesting that the mathematical formalization of the data set generating process, does improve the *TimeWave* accuracy.

Another significant feature of the revised data correlation plot in Fig. 20 that should be mentioned here, is the fact that the correlation coefficient for the 1915 period is nearly - 1, signifying an anti-correlation or mirror image relationship between the waves. This is

the TimeWave comparison that is shown in Fig. 18. If one were to place an imaginary two-sided mirror between the standard and revised TimeWave graphs, then the reflection on either side of the mirror would closely resemble the wave that is on the other side – hence the description of anti-correlation as a mirror image relationship. Also notice, that a green dotted line marks the average of all the standard/revised wave correlations at about 70%.

The red line of Fig. 20 shows the correlation of the random number generated waves, with the standard data set. By definition, the random data sets should show little or no correlation with either the standard or revised data sets, nor with any other random number set. In several cases in Fig. 20, this turns out to be true, but there are also several cases in which the random set correlation is not near zero, as one would expect. In general, the red line plot of Fig. 20 shows a much lower level of correlation with the *standard* number set than does the *revised* set – as expected. Each data point on the red line, however, is actually an average of either two, or seven random number set correlations. In other words, either two or seven random number correlations were averaged to produce each point on the red line graph. It turns out that most of the sixteen correlation points produced by averaging only two random sets, have much more scatter than do the four points produced by averaging seven random set correlations. The 384 number *random data set*, and the periods 1895-1925, 1905, and 1915, were all produced by averaging seven random set correlations. The violet dotted line running through the random number set correlations, is the average correlation level for all the random sets shown, and it shows a very low average correlation of about 5%.

It is also possible that the same process proposed for producing the larger correlation scatter of the revised data set, could be at work for the random data sets – i.e. short duration time periods with low sampling frequencies, could be causing data scatter due to noise. If a small number of the 384 *data file* points are used to generate a *short period TimeWave*, then there is a much higher probability of correlation between the random sets and the TimeWave number sets. Without further investigation, however, this is a speculative, if plausible thesis.

The graphs of Fig. 20 do show that the *standard* and *revised* data sets and their derivative *TimeWaves* are remarkably well correlated. In the regions where the correlation weakens, or breaks down entirely, the revised *TimeWave* appears to show a Novelty process that is in closer agreement with known historical process. In addition, the plots in Fig. 20 may be revealing a process whereby short period *TimeWaves* produce sampling noise that weakens the correlation. This data supports the view, that the information content of the *standard TimeWave* is somewhat distorted, but not destroyed; and suggests that the *revised TimeWave* and its *piecewise linear function* is able to correct this distortion, and provides an improved expression of the Novelty process.

## Concluding Remarks

The development of the 384 number *data set* from the set of *First Order of Difference* (FOD) integers has been expressed as a process that is *piecewise linear* in nature. This process involves the combination and expansion of straight-line segments, which can be

expressed mathematically as a *piecewise linear function*. The *standard development* has been described by McKenna and Meyer in the *TimeWave Zero* documentation and in other reports. But this process includes a procedural step called the “half twist”, that is not consistent with the structure of piecewise linear mathematics; and consequently produces a distortion of the FOD information content. Watkins elaborated on this in some detail, in his well-documented expose on the nature of the *half twist*, in which he described the distortions and inconsistencies involved. He then concluded that this distortion would render the *TimeWave* meaningless, as a realistic graphical depiction of the *Novelty* process as had been described by McKenna. I maintain that this conclusion was premature, and apparently incorrect.

The *revised development* of the 384 number *data set* includes the use of mathematics that correctly expresses the *piecewise linear* development process, and therefore produces an undistorted expansion of the FOD number set. The *TimeWave* that results from this expansion process, is then an accurate reflection of the FOD number set, provided the set can be described or modeled by a piecewise linear function. The *piecewise linear function* described here, may only be an approximation to some more *complex function* that has yet to be found. In fact, I would argue that this is quite likely for a phenomenon or process of this nature, which further study may shed some light on. If we assume that the *revised TimeWave* is a reasonably accurate reflection of the information content of the FOD number set, then the *standard TimeWave* should have a degree of accuracy proportional to its degree of correlation with the *revised TimeWave*. As we have seen thus far, these two *TimeWaves* show an *average correlation* of about 70%, so that the *standard wave* has an average accuracy of about 70% when compared with the *revised wave*. However, we have also seen this correlation as high as 98%, or as low as 6%, with one case of a mirror image or anti-correlation of  $-0.94$ .

This work has served to clarify and formalize the process by which the 384 number *TimeWave data set* is generated. This has been done by showing that the process is describable within the framework of piecewise linear mathematics in general, and vector mathematics in particular. Each step has been delineated and formalized mathematically, to give the process clarity and continuity. The formalized and revised data set serves as the foundation of the *TimeWave* generated by the *TimeWave Zero* software, which is viewed as a graphical depiction of a process described by the ebb and flow of a phenomenon called *Novelty*. *Novelty* is thought to be the basis for the creation and conservation of higher ordered states of complex form in nature and the universe.

The results reported here make no final claims as to the validity of the *TimeWave* as it is expressed by *Novelty Theory*, nor does it claim that the current *TimeWave* is the best description of this *Novelty* process. It does show that the proper mathematical treatment of the FOD number set, produces a *TimeWave* that appears to be more consistent with known historical process. This consistency is general, however, and more work needs to be done to examine the specific reflections or projections that the *TimeWave* may be revealing. If *Novelty Theory* is a valid hypothesis, reflecting a real phenomenon in nature, then one would expect that it is verifiable in specific ways.

It has also seemed appropriate to examine some of the steps in this wave development process in terms of their correspondence with elements of philosophy and science. The

flow of Yin and Yang energy reflected in the expression of the forward and reverse bi-directional waves, for example, finds philosophical correspondence in a natural cycle of life-death-rebirth, or in the process of the shamanic journey – immersion, engagement, and return. Correspondence can also be found in science, in the fields of cosmology, astronomy, astrophysics, and quantum physics – the life cycles and motion of heavenly bodies, quarks, and universes; the harmonic and holographic nature of light and wave mechanics; and the cyclic transformation of matter to energy, and energy to matter. The reflection of all natural phenomena and processes over the continuum of existence, from the smallest scales up to the largest scales, must surely include whatever process is occurring in the I-Ching as well. The question is, are we are clever and conscious enough to decipher and express it correctly and appropriately?

## Acknowledgements

I would like to thank [Terence McKenna](#), for bringing this intriguing and provocative notion into the collective, and for the courage and foresight shown, by his willingness to open himself and his ideas to scrutiny and boundary dissolution. If there is any relevance or meaning to be found in the *TimeWave* or *Novelty Theory*, then it is surely something that is larger than he, or any of us; and it is also something that is properly in the domain of all human experience, with each of us a witness, participant, and contributor.

I would also like to express my thanks and appreciation to [Mathew Watkins](#) for his work in exposing the mathematical inconsistencies, vagaries, and procedural errors of the standard *TimeWave data set* development, and challenging a theory that may have become far too sedentary and inbred for its own good. Whatever the final outcome of this endeavor of *Novelty Theory*, he has set the enterprise on its proper course of open and critical inquiry.

I am also greatly indebted to [Peter Meyer](#) for his skill and foresight in creating a TWZ software package that is flexible, accessible, and friendly to the serious investigator. Without his DOS version of TimeWave Zero software, this work would have been much more difficult if not impossible. He has created a software package that makes these notions realistically testable, in a relatively straightforward manner. This made it possible for me to examine the effects of the revised data set on the TimeWave itself, as well as facilitating the examination of the detailed structure of the wave in work to follow.

My thanks also to [Dan Levy](#) for his offer to publish this work on his [Levity](#) site, as well as hosting an upcoming *TimeWave* mathematical annex to *Novelty Theory*. I want also to acknowledge [Brian Crissey](#) at [Blue Water Publishing](#) for his help in integrating the new process into the TimeWave Zero software packages and documentation.

---

<sup>1</sup> Computer Software program written by Meyer and others, based on a mathematical relationship exhibited by the I-Ching, formulated and reported by T. McKenna and D. McKenna, *the Invisible Landscape*, Harper San Francisco, 1993, p. 121

<sup>2</sup> T. McKenna, *the Invisible Landscape*, p. 140

<sup>3</sup> M. Watkins, *Autopsy for a Mathematical Hallucination*, Terence McKenna's Hyperborea at [www.levity.com](http://www.levity.com)

- 
- <sup>4</sup> T. McKenna, *Time Explorer* Manual, p60, the Invisible Landscape, pp. 140-142
- <sup>5</sup> P. Meyer, <http://www.magnet.ch/serendipity/twz/kws.html>
- <sup>6</sup> DeltaPoint, Inc., 22 Lower Ragsdale Dr., Monterey, CA 93940, (408) 648-4000
- <sup>7</sup> Microsoft Corp., One Microsoft Way, Redmond, WA 98052
- <sup>8</sup> McKenna, *TimeExplorer* Manual, PP. 60-63, <http://www.levity.com/eschaton/waveexplain.html>
- <sup>9</sup> H.B. Anderson, *Analytic Geometry with Vectors*, p71, McCutchan Publishing Corp., Berkeley, Ca. 1966
- <sup>10</sup> T. McKenna, *TimeExplorer* software manual, pp. 62-63
- <sup>11</sup> P. Meyer, *TimeExplorer* software manual, pp. 85-91
- <sup>12</sup> M. Kaku, *What Happened BEFORE the Big Bang?*, *Astronomy*, May 1996, pp. 34-41

[\[John Sheliak\]](#) [sheliak@dsrt.com](mailto:sheliak@dsrt.com)

[\[Terence McKenna\]](#) [syzygy@ultraconnect.com](mailto:syzygy@ultraconnect.com)

[\[return to Levity\]](#) <http://www.levity.com/eschaton/>



Filename: MathWave PaperII  
Directory: D:\DG4\TWZ Files  
Template: C:\Program Files\Microsoft  
Office\Templates\NORMAL.DOT  
Title: Delineation, Specification, and Formalization of the TWZ  
Data Set Generation Process - Philosophical, Procedural, and Mathematical  
Subject:  
Author: John Sheliak  
Keywords:  
Comments:  
Creation Date: 11/11/97 9:50 PM  
Change Number: 2  
Last Saved On: 11/11/97 9:50 PM  
Last Saved By: John Sheliak  
Total Editing Time: 1 Minute  
Last Printed On: 11/11/97 9:51 PM  
As of Last Complete Printing  
Number of Pages: 48  
Number of Words: 13,802 (approx.)  
Number of Characters: 78,672 (approx.)